# New analysis of SNeIa Pantheon Catalog: Variable speed of light as an alternative to dark energy

Hoang Ky Nguyen\*

Department of Physics, Babeş-Bolyai University, Cluj-Napoca 400084, Romania Institute for Interdisciplinary Research in Science and Education, ICISE, Quy Nhon 55121, Vietnam (Dated: March 12, 2025)

In A&A 412, 35 (2003) Blanchard, Douspis, Rowan-Robinson, and Sarkar (BDRS) slightly modified the primordial fluctuation spectrum and produced an excellent fit to WMAP's CMB power spectrum for an Einstein-de Sitter (EdS) universe, bypassing dark energy. Curiously, they obtained a Hubble value of  $H_0 \approx 46$ , in sharp conflict with the canonical range  $\sim 67-73$ . However, we will demonstrate that the reduced value of  $H_0 \approx 46$  achieved by BDRS is fully compatible with the use of variable speed of light in analyzing the late-time cosmic acceleration observed in Type Ia supernovae (SNeIa). In Phys. Lett. B 862 (2025) 139357 we considered a generic class of scale-invariant actions that allow matter to couple non-minimally with gravity via a dilaton field  $\chi$ . We discovered a hidden aspect of these actions: the dynamics of the dilaton can induce a variation in the speed of light c as  $c \propto \chi^{1/2}$ , thereby causing c to vary alongside  $\chi$  across spacetime. For an EdS universe with varying c, besides the effects of cosmic expansion, light waves emitted from distant SNeIa are further subject to a refraction effect, which alters the Lemaître redshift relation to  $1+z=a^{-3/2}$ . Based on this new formula, we achieve a fit to the SNeIa Pantheon Catalog exceeding the quality of the  $\Lambda$ CDM model. Crucially, our approach does not require dark energy and produces  $H_0 = 47.2 \pm 0.4$ (95% CL) in strong alignment with the BDRS finding of  $H_0 \approx 46$ . The reduction in  $H_0$  in our work, compared with the canonical range  $\sim 67-73$ , arises due to the 3/2-exponent in the modified Lemaître redshift formula. Hence, BDRS's analysis of the (early-time) CMB power spectrum and our variable-c analysis of the (late-time) Hubble diagram of SNeIa fully agree on two counts: (i) the dark energy hypothesis is avoided, and (ii)  $H_0$  is reduced to  $\sim 47$ , which also yields an age  $t_0 = 2/(3H_0) = 13.8 \,\mathrm{Gy}$  for an EdS universe, without requiring dark energy. Most importantly, we will demonstrate that the late-time acceleration can be attributed to the declining speed of light in an expanding EdS universe, rather than to a dark energy component.

## I. MOTIVATION

The  $\Lambda$ CDM model serves as the standard framework for modern cosmology, efficiently accounting for a wide range of astronomical observations. While the model is widely regarded as successful, it faces significant challenges [1]. Notably, ongoing tensions in the determination of the Hubble constant  $H_0$  and the amplitude of matter fluctuations  $\sigma_8$  raise questions about the underpinning principles of the model [2]. Moreover, an integral component of this model is dark energy (DE), which constitutes approximately 70% of the total energy budget of the universe. The nature of DE itself—along with its finetuning and coincidence problems—poses profound challenges both in cosmology and in the broader context of field theories [3].

In 2003, Blanchard, Douspis, Rowan-Robinson, and Sarkar (BDRS) proposed a novel approach to mitigate the need for DE when analyzing the cosmic microwave background (CMB) power spectrum [4]. They relied on the Einstein–de Sitter universe, which corresponds to the flat  $\Lambda$ CDM model with  $\Omega_{\Lambda}=0$ . Instead of the conventional single-power primordial fluctuation spectrum,

 $P(k) = Ak^n$ , they employed a double-power form

$$P(k) = \begin{cases} A_1 k^{n_1} & k \leq k_* \\ A_2 k^{n_2} & k \geqslant k_* \end{cases}$$
 (1)

with continuity imposed across the breakpoint  $k_*$ . Remarkably, this modest modification produced an excellent fit to the CMB power spectrum without invoking DE. In [5], Hunt and Sarkar further developed a supergravity-based inflation scenario to validate the double-power form given in Eq. (1) and also attained an excellent fit while avoiding DE. The works by BDRS and the Hunt–Sarkar team—if correct—would seriously undermine the viability of the DE hypothesis.

Surprisingly, the fit by BDRS yielded a new value of  $H_0 \approx 46$ , while the fit by Hunt and Sarkar produced a comparable value of  $H_0 \approx 44$ . Obviously, these values are at odds with the value of  $H_0 \sim 70$  derived from the Hubble diagram of Type Ia supernovae (SNeIa), based on the  $\Lambda$ CDM model with  $\Omega_{\Lambda} \approx 0.7$ . Since DE has been regarded as the driving force of the late-time cosmic acceleration, interest in the works by BDRS and the Hunt–Sarkar team has largely diminished in favor of the standard  $\Lambda$ CDM model.

Amid this backdrop, we will reexamine the SNeIa data in the context of a cosmology that supports a varying

<sup>\*</sup> hoang.nguyen@ubbcluj.ro

speed of light c on an expanding EdS cosmic background, rather than the  $\Lambda$ CDM model. Recently, the theoretical foundation for a varying c in spacetime has been derived, using a class of scale-invariant actions that enable non-minimal coupling of matter with gravity via a dilaton field [6, 7]. In cosmology, a varying c should impact the propagation of light rays from distant SNeIa to an Earth-based observer, fundamentally altering the distance-vs-redshift relationship. This modification necessitates a re-evaluation of the  $H_0$  value derived from the Hubble diagram of SNeIa, potentially replacing the canonical value  $\sim$  70 that relies on the  $\Lambda$ CDM model.

The purpose of our paper is two-fold: (i) to investigate the viability of the variable speed of light (VSL) theory developed in Refs. [6, 7] in accounting for the late-time cosmic acceleration while bypassing DE, and (ii) to determine whether—and how—the finding of  $H_0 \approx 46$  by BDRS for the CMB can be reconciled with our reexamination of SNeIa in the VSL context.

Our paper is organized into four major parts:

- \* Foundation of VSL: Section II covers the history of VSL and provides a recap of our mechanism for generating varying c, as presented in [6, 7].
- \* Cosmography of VSL: Sections III and IV prepare the foundational material necessary for cosmography in the presence of varying c. Section V develops various modified redshift relations—Lemaître, distance vs. z, and luminosity distance vs. z—by incorporating variations in the speed of light. Importantly, we derive a modified Hubble law, applicable to our VSL scheme.
- \* Cosmology of VSL: Section VI presents our analysis of the Combined Pantheon Sample of SNeIa data using our modified luminosity distance vs. redshift formula derived in the preceding sections.
- \* Consequences of VSL: We aim for four objectives: (i) Section VII presents a new interpretation of the accelerating expansion through varying c instead of DE; (ii) Section VIII revisits BDRS's analysis of the CMB power spectrum without requiring DE and reconcile it with our findings from the VSL-based analysis of SNeIa; (iii) Section IX resolves the age problem without using DE; and (iv) Section X offers a potential resolution to the  $H_0$  tension from an astronomical origin while avoiding dynamical DE.

Section XI discusses and summarizes our findings, and the appendices contain technical supplements.

# II. A NEW MECHANISM TO GENERATE VARYING C FROM DILATON DYNAMICS

The variability in the speed of light was first recognized by Einstein in 1911 during his pursuit for a generally covariant theory of gravitation, which ultimately culminated in the theory of General Relativity (GR) in 1915. In Ref. [8] he explicitly allowed the gravitational

field  $\Phi$  to influence the value of c in spacetime. In particular, he proposed that  $c = c_0 (1 + \Phi/c^2)$ , where  $c_0$  is the speed of light at a reference point where  $\Phi$  vanishes. Notably, he conceived this radical idea six years after his formulation of Special Relativity (SR). As Einstein emphasized in [9, 10], a variation in c does not contradict the principle of the constancy of c under Lorentz transformations, an underpinning requirement of SR. This is because Lorentz invariance, confirmed by the Michelson-Morley (MM) experiment, is only required to hold in *local* inertial frames and does not necessitate its global validity in curved spacetimes. More concretely, in a region vicinity to a given point  $x^*$ , the tangent frames to the spacetime manifold possess the Lorentz symmetry with a common value of c applicable only to that region. Yet, in a spacetime influenced by a gravitational field, different regions can—in principle—correspond to different values of c. Utilizing the language of Riemannian geometry, the speed of light can be promoted to a scalar field: while cis an *invariant* (i.e., unaffected upon diffeomorphism), it can nonetheless be position-dependent, viz.  $c(x^*)$ .

Einstein's pioneering concept of VSL, nevertheless, was quickly overshadowed by the success of his GR and subsequently fell into dormancy for several decades. The variability of c was briefly rediscovered by Dicke in 1957 [11], prior to his own development of Brans–Dicke gravity [12], which instead allowed Newton's gravitational constant G to vary. In the 1990s, the idea of VSL was independently revived by Moffat [13] and by Albrecht and Magueijo [14] in the context of early-time cosmology. Their proposals aimed to resolve the horizon puzzle while avoiding the need for cosmic inflation. Since then, several researchers actively explore various aspects of VSL [15–88].

In a recent report [6], we considered a scale-invariant action that facilitates non-minimal coupling of matter with gravity via a dilaton field  $\chi$ . We uncovered a hidden mechanism that induces a dependence of c and  $\hbar$  on the dilaton field  $\chi$ , thereby causing c and  $\hbar$  to vary alongside  $\chi$  in spacetime. Below is a recap of our mechanism.

# The essence of our VSL mechanism

Let us consider a prototype action:

$$S = \int d^4x \sqrt{-g} \left[ \mathcal{L}_{\text{grav}} + \mathcal{L}_{\text{mat}} \right]$$
 (2)

$$\mathcal{L}_{\text{grav}} = \chi^2 \, \mathcal{R} - 4\omega g^{\mu\nu} \, \partial_{\mu} \chi \partial_{\nu} \chi \tag{3}$$

$$\mathcal{L}_{\text{mat}} = i \, \bar{\psi} \gamma^{\mu} \nabla_{\mu} \psi + \sqrt{\alpha} \, \bar{\psi} \gamma^{\mu} A_{\mu} \psi + \mu \, \chi \, \bar{\psi} \psi - \frac{1}{4} F_{\mu\nu} F^{\mu\nu}$$
(4)

The gravitational sector  $\mathcal{L}_{grav}$  is equivalent to the well-known Brans–Dicke theory,  $\mathcal{L}_{BD} = \phi \mathcal{R} - \frac{\omega}{\phi} g^{\mu\nu} \partial_{\mu} \phi \partial_{\nu} \phi$ , upon substituting  $\phi := \chi^2$  [12]. The matter Lagrangian  $\mathcal{L}_{mat}$  describes quantum electrodynamics (QED) for an electron field  $\psi$ , coupled with an electromagnetic field  $A_{\mu}$ 

(with the field tensor defined as  $F_{\mu\nu} := \partial_{\mu}A_{\nu} - \partial_{\nu}A_{\mu}$ ) and embedded in a curved spacetime characterized by the metric  $g^{\mu\nu}$ . The Dirac gamma matrices satisfy  $\gamma^{\mu}\gamma^{\nu} + \gamma^{\nu}\gamma^{\mu} = 2g^{\mu\nu}$ , and the spacetime covariant derivative  $\nabla_{\mu}$  acts on the spinor via vierbein and spin connection. However, the electron field couples non-minimally with gravity via the dilaton field, viz.  $\chi \bar{\psi}\psi$ .

All parameters  $\alpha$ ,  $\mu$ , and  $\omega$  are dimensionless. The full action is scale invariant, viz. unchanged under the global Weyl rescaling

$$g_{\mu\nu} \to \Omega^2 g_{\mu\nu}; \ \chi \to \Omega^{-1} \chi; \ \psi \to \Omega^{-\frac{3}{2}} \psi; \ A_\mu \to A_\mu$$
 (5)

It has been established in [89, 90] that a scale-invariant action, such as the one described in Eqs. (6)–(8), can evade observational constraints on the fifth force.

Next, let us revisit the 'canonical' QED action for an electron field  $\psi$  carrying a U(1) gauge charge e and inertial mass m, coupled with an electromagnetic field  $A_{\mu}$  and embedded in an Einstein–Hilbert spacetime

$$S_0 = \int d^4x \sqrt{-g} \left[ \mathcal{L}_{EH} + \mathcal{L}_{QED} \right]$$
 (6)

$$\mathcal{L}_{\rm EH} = \frac{c^3}{16\pi\hbar G} \,\mathcal{R} \tag{7}$$

$$\mathcal{L}_{\text{QED}} = i \, \bar{\psi} \gamma^{\mu} \nabla_{\mu} \psi + \frac{e}{\sqrt{\hbar c}} \bar{\psi} \gamma^{\mu} A_{\mu} \psi + m \frac{c}{\hbar} \, \bar{\psi} \psi - \frac{1}{4} F_{\mu\nu} F^{\mu\nu}$$
(8)

In these expressions, the quantum of action  $\hbar$ , speed of light c, and Newton's gravitational parameter G are explicitly restored.

Excluding the kinetic term  $g^{\mu\nu}\partial_{\mu}\chi\partial_{\nu}\chi$  of the dilaton in Eq. (3), the action  $\mathcal{S}$  can be brought into the form  $\mathcal{S}_0$  via the following identification:

$$\frac{c^3}{16\pi\hbar G} := \chi^2; \quad \frac{e}{\sqrt{\hbar c}} := \sqrt{\alpha}; \quad m\frac{c}{\hbar} := \mu \chi \qquad (9)$$

These identities link the charge e and inertial mass m of the electron with the three 'fundamental constants' c,  $\hbar$ , and G, as well as the dilaton field  $\chi$ .

To proceed, we require that the intrinsic properties of the electron—namely, its charge e and inertial mass m—remain independent of the background spacetime, particularly the dilation field  $\chi$  which belongs to the gravitational sector. Consequently, based on the last two identities of Eq. (9), both the speed of light c and the quantum of action  $\hbar$  must be treated as scalar fields related to  $\chi$ . The following assignments capture this relationship:

$$c_{\chi} := \hat{c} \left(\frac{\chi}{\hat{\chi}}\right)^{1/2}; \quad \hbar_{\chi} := \hat{h} \left(\frac{\chi}{\hat{\chi}}\right)^{-1/2}$$
 (10)

Here, the subscript  $\chi$  signifies the dependence of c and  $\hbar$  on  $\chi$ , while  $\hat{c}$  and  $\hat{h}$  represent the values of  $c_{\chi}$  and  $\hbar_{\chi}$ 

at a reference point where  $\chi = \hat{\chi}$  (with  $\hat{\chi} \neq 0$ ). It is straightforward to derive from Eqs. (9) and (10) that

$$e = \left(\alpha \hat{h}\hat{c}\right)^{1/2}; \quad m = \frac{\mu \hat{h}\hat{\chi}}{\hat{c}}; \quad G = \frac{\hat{c}^3}{16\pi \hat{h}\hat{\chi}^2}$$
 (11)

This confirms that e and m are indeed constants <sup>1</sup>. Furthermore, G is also constant.

As the dilaton  $\chi$  varies in spacetime as a component of the gravitational sector, the scalar fields  $c_{\chi}$  and  $\hbar_{\chi}$ , defined in Eq. (10), also vary in spacetime. Therefore, the dynamics of the dilaton  $\chi$  induces variations in  $c_{\chi}$  and  $\hbar_{\chi}$  on the spacetime manifold.

#### Comments on Brans–Dicke's variable G

Traditionally, Brans–Dicke (BD) gravity is associated with variable Newton's gravitational constant G [12]. It should be noted that Brans and Dicke only allowed matter to couple minimally with gravity, namely, through the 4–volume element  $\sqrt{-g}$ ; in this case, the matter action is not scale invariant. To achieve scale invariance, matter must couple with gravity in a non-minimal way, such as the Lagrangian given in Eq. (4). In this case, if one presumes that c and  $\hbar$  are constants, then the mass parameters of (massive) fields also become variable [91–94].

Indeed, under the assumption of constant c and  $\hbar$ , Eq. (9) readily produces

$$e = (\alpha \hbar c)^{1/2}; \quad m_{\chi} = \frac{\mu \hbar}{c} \chi; \quad G_{\chi} = \frac{c^3}{16\pi \hbar} \chi^{-2}$$
 (12)

Here, the subscript  $\chi$  signifies the dependence of m and G on  $\chi$ . In [6], we referred to these results as "the Fujii–Wetterich scheme", since these authors appear to be the first to report results (in [91–94]) essentially equivalent to Eq. (12). In this scheme, while m is associated with  $\chi$ , the charge e remains independent of  $\chi$ , rendering an unequal treatment of e and e Moreover, whereas e affects the electron's mass per Eq. (12), massless particles, such as photons, remain unaffected.

Our mechanism thus represents a significant departure from the variable G (and mass) approach. Importantly, it allows the dilaton  $\chi$ —through its influence on the speed of light  $c_{\chi}$  and quantum of action  $\hbar_{\chi}$ —to govern the propagation and quantization of all fields—viz. electron and photon—on a universal and equal basis.

While both approaches—(i) variable G and m versus (ii) variable c and  $\hbar$ —are mathematically permissible, they are *not physically equivalent* [6], and the validity of each approach should be determined through empirical

 $<sup>^{1}</sup>$  Note: When radiative corrections in the matter sector are taken into account, e and m can 'run' in the renormalization group flow as functions of the momentum level at which they are measured.

evidence, including predictions, experiments and observations.

Our mechanism leads to a direct and immediate consequence in cosmology, however. Specifically, the aspect of our mechanism where the dynamical  $\chi$  induces a variation in  $c_{\chi}$ , which in turn governs massless field (viz. the light quanta) has significant implications. A varying c influences the propagation of light rays emitted from distant sources toward an Earth-based observer, thereby affecting the Hubble diagram of these light sources, particularly for SNeIa. This intuition serves as the underpinning for the analysis presented in the remainder of this paper.

### Scaling properties of length, time, and energy

In [6] we further deduced that at a given point  $x^*$ , the prevailing value of the dilaton  $\chi(x^*)$  determines the lengthscale, timescale, and energy scale for physical processes occurring at that point. The lengthscale l and energy scale E are dependent on  $\chi$  as follows

$$l \propto \chi^{-1}; \quad E \propto \chi.$$
 (13)

However, the most important outcome is that the timescale  $\tau$  behaves in an anisotropic fashion, as

$$\tau \propto \chi^{-3/2} \tag{14}$$

or, equivalently

$$\tau \propto l^{3/2} \,. \tag{15}$$

This leads to a novel time dilation effect induced by the dilaton, representing a concrete prediction of our mechanism. Moreover, the 3/2–exponent in this time scaling law plays a crucial role in the Hubble diagram of SNeIa, as we will explore in the following sections.

A detailed exposition of our mechanism and the new time dilation effect is presented in Ref. [6].

# III. IMPACTS OF VARYING C IN AN EINSTEIN-DE SITTER UNIVERSE

In a cosmology accommodating VSL, as a lightwave travels from a distant SNeIa toward an Earth-based observer, a varying speed of light along its trajectory induces a refraction effect akin to that experienced by a physical wave traveling through an inhomogenous medium with varying wave speed. The alteration of the wavelength results in a new set of cosmographic formulae, including a modified Hubble law and a modified relationship between redshift and luminosity distance.

# A. A drawback in previous VSL analyses of SNeIa

It is important to note that since the revival of VSL by Moffat and the Albrecht–Magueijo team in the 1990s, several authors have applied VSL to late-time cosmology, particularly in the analysis of the Hubble diagram of SNeIa. However, these attempts have not met with much success [15, 16, 34–38]. A common theme among these analyses is the assumption that cvaries as a function of the global cosmic factor a of the Friedmann-Lemaître-Roberson-Walker (FLRW) metric (e.g., in the form  $c \propto a^{-\zeta}$  first proposed by Barrow [15]). These works generally conclude that, despite the dependence of c on a, VSL does not alter the classic Lemaître redshift formula  $1+z=a^{-1}$  and, therefore, cannot play any role in the Hubble diagram of SNeIa. However, upon closer scrutiny into these works, we identify a significant oversight: they implicitly assumed that c is a function solely of cosmic time t, through the dependence of a on t in the FLRW metric. This assumption is not valid in our VSL framework, where c—through its dependence on the dilaton field  $\chi$  varies in both *space* and time, rather than time alone. In this section, as well as Sections IV and V, we will demonstrate that the variation of c as a function of the dilaton field  $\chi$ , rather than merely as a function of the cosmic factor (viz. a) as assumed in prior VSL works, fundamentally alters the Lemaître redshift formula and necessitates a re-analysis of SNeIa data.

## B. The modified FLRW metric

The FLRW metric for the isotropic and homogeneous intergalactic space reads

$$ds^{2} = c^{2}dt^{2} - a^{2}(t) \left[ \frac{dr^{2}}{1 - \kappa r^{2}} + r^{2}d\Omega^{2} \right]$$
 (16)

where a(t) is the global cosmic scale factor that evolves with cosmic time t.

Our goal is to investigate whether an Einstein–de Sitter universe, when supplemented with a varying c, can account for the Hubble diagram of SNeIa as provided by the Pantheon Catalog. We will make three working assumptions:

**Assumption** #1: The FLRW universe is spatially flat, corresponding to  $\kappa = 0$ . There is robust observational evidence supporting this assumption.

Assumption #2: The cosmic scale factor evolves as

$$a = a_0 \left(\frac{t}{t_0}\right)^{2/3} \tag{17}$$

Justification: In our VSL mechanism, the timescale  $\tau$  and lengthscale l of a given physical process are related

by  $\tau \propto l^{3/2}$ , as expressed in Eq. (15). Regarding the evolution of the FLRW metric, its timescale and lengthscale can be identified with t and a, respectively. The growth law given in Eq. (17) is therefore justified. Note: This growth is identical to the evolution of an EdS universe, viz. a spatially flat, expanding universe consisting solely of matter, with no contribution from DE or a cosmological constant.

Assumption #3: The dilaton field in the cosmic background depends on the cosmic factor in the form

$$\chi \propto a^{-1} \,. \tag{18}$$

Justification: In our VSL mechanism, the lengthscale of a given physical process is inversely proportional to the dilaton field, per Eq. (13). Given that the cosmic factor a plays the role of the lengthscale for the FLRW metric, the dependency expressed in Eq. (18) is therefore justified.

Combining Eqs. (10) and (18) then renders  $c \propto a^{-1/2}$ , or more explicitly

$$c = c_0 \left(\frac{a}{a_0}\right)^{-1/2} \tag{19}$$

Here,  $a_0$  is the current cosmic scale factor (often set equal 1), and  $c_0$  is the speed of light measured at our current time in the intergalactic space. We should emphasize that the value of  $c_0$  is not identical with the one measured *inside the Milky Way*, which is equal to 300,000 km/s. This is because the Milky Way is a gravitationally bound structure whereas the intergalactic space is regions subject to cosmic expansion. This issue will be explained in Section IV.

Combining Eqs. (16) and (19), and setting  $\kappa = 0$ , we then obtain the *modified* FLRW metric

$$ds^{2} = \frac{c_{0}^{2}a_{0}}{a(t)} dt^{2} - a^{2}(t) \left[ dr^{2} + r^{2} d\Omega^{2} \right]$$
 (20)

which describes an EdS universe with a declining speed of light, per  $c \propto a^{-1/2}$ .

## C. Frequency shift

For the modified FLRW metric derived above, the null geodesic  $(ds^2=0)$  for a lightwave traveling from a distant emitter toward Earth (viz.  $d\Omega=0$ ) is

$$c_0 a_0^{1/2} \frac{dt}{a^{3/2}(t)} = dr (21)$$

Hereafter, we will use the subscripts "em" and "ob" for "emission" and "observation" respectively. Denote  $t_{em}$  and  $t_{ob}$  the emission and observation time points of the lightwave, and  $r_{em}$  the co-moving distance of the emitter from Earth. From (21), we have:

$$c_0 a_0^{1/2} \int_{t_{em}}^{t_{ob}} \frac{dt}{a^{3/2}(t)} = r_{em}$$
 (22)

The next wavecrest to leave the emitter at  $t_{em} + \delta t_{em}$  and arrive at Earth at  $t_{ob} + \delta t_{ob}$  satisfies:

$$c_0 a_0^{1/2} \int_{t_{em} + \delta t_{em}}^{t_{ob} + \delta t_{ob}} \frac{dt}{a^{3/2}(t)} = r_{em}$$
 (23)

Subtracting these two equations yields:

$$\frac{\delta t_{ob}}{a^{3/2}(t_{ob})} = \frac{\delta t_{em}}{a^{3/2}(t_{em})} \tag{24}$$

which leads to the ratio between the emitted frequency and the observed frequency:

$$\frac{\nu_{ob}}{\nu_{em}} = \frac{\delta t_{em}}{\delta t_{ob}} = \frac{a^{3/2}(t_{em})}{a^{3/2}(t_{ob})} = \left(\frac{a_{em}}{a_{ob}}\right)^{3/2} \tag{25}$$

This contrasts with the standard relation,  $\frac{\nu_{ob}}{\nu_{em}} = \frac{a_{em}}{a_{ob}}$ . To derive a Lemaître formula applicable for VSL, further consideration is needed. This task will be carried out in the next section.

## IV. IMPACTS OF VARYING C ACROSS BOUNDARIES OF GALAXIES

This section presents the pivotal elements that enable the 3/2-exponent in the frequency ratio, as expressed in Eq. (25), to manifest in observations.

# A. The loss of validity of Lemaître formula

Let us first revisit the drawback in previous VSL works alluded to in Section III A. The frequency ratio given by Eq. (25) can be converted into the wavelength ratio

$$\frac{\lambda_{ob}}{\lambda_{em}} = \frac{c_{ob}}{c_{em}} \cdot \frac{\nu_{em}}{\nu_{ob}} = \frac{a_{ob}^{-1/2}}{a_{em}^{-1/2}} \cdot \frac{a_{ob}^{3/2}}{a_{em}^{3/2}} = \frac{a_{ob}}{a_{em}}$$
(26)

This expression is exactly *identical* to that in standard cosmology, viz. where c is non-varying. At first, it may seem tempting to relate the redshift z with  $\frac{\lambda_{ob} - \lambda_{em}}{\lambda_{em}}$ , namely

$$1 + z \stackrel{?}{=} \frac{\lambda_{ob}}{\lambda_{em}} = \frac{a_{ob}}{a_{em}} = a^{-1}$$
 (27)

in which  $a_{ob}$  is set equal 1 and  $a_{em}$  is denoted as a. In Refs. [16, 34–38], based on Eq. (27), it was concluded that the classic Lemaître redshift formula,  $1+z=a^{-1}$ , remained valid. Subsequently, virtually all empirical VSL works continued using the classic Lemaître formula to analyze the Hubble diagram of SNeIa.

However, the formula in Eq. (27) is *incorrect*. One key reason is that  $\lambda_{ob}$ , representing the wavelength in the intergalactic space enclosing the Milky Way, is *not* what the Earth-based astronomer directly measures. For the light wave to reach the astronomer's telescope, it

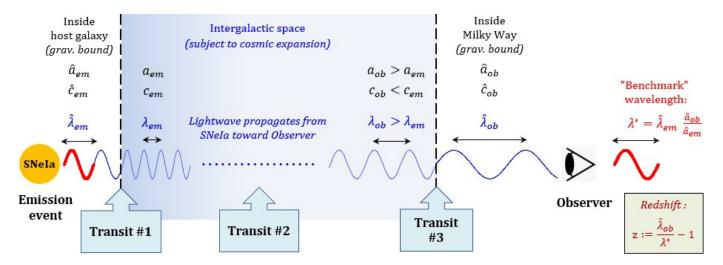


Figure 1. A lightwave from an SNeIa explosion (shown on the far left) makes three transits to reach the Earth-based astronomer (shown on the far right). During Transit #1, the lightwave exits the (gravitationally-bound) host galaxy to enter the surrounding intergalactic region; the wavecrest gets compressed as light speed decreases at this juncture. During Transit #2, the lightwave travels in the intergalactic space which undergoes cosmic expansion; accordingly, the wavecrest expands. During Transit #3, the lightwave enters the (gravitationally-bound) Milky Way; the wavecrest expands further as light speed increases at this juncture. The Earth-based astronomer measures the wavelength  $\hat{\lambda}_{ob}$  and compares it with the "benchmark" wavelength  $\lambda^*$  (see text for explanation) to calculate the redshift z (shown in the lower right corner box).

must pass through the gravitationally-bound Milky Way, which has its own local scale  $\hat{a}_{ob}$  differing from the current global cosmic scale because the matter-populated Milky Way resists cosmic expansion. This crucial point will be clarified shortly in the section below. In brief, a change in scale (from global to local) across the boundary of the Milky Way induces a corresponding change in the speed of light. This effect alters the wavelength from  $\lambda_{ob}$  to  $\hat{\lambda}_{ob}$  which is then measured by the astronomer.

# B. Refractive effect due to varying c across boundaries of galaxies

The global cosmic scale factor a grows with comic time t, leading to the stretching of wavelength of light from  $\lambda_{em}$  to  $\lambda_{ob}$ . However, the Solar System is not subject to cosmic expansion, which is a crucial condition so that the Earth-based observer can detect the redshift of distant emission sources. It is well understood that if the Solar System expanded along with the intergalactic space, the observer's instruments would also expand in sync with the wavelength of the light ray emitted from a distant supernova, making the detection of any redshift impossible. More generally, mature galaxies—those hosting distant SNeIa, and the Milky Way where the Earth-based observer resides, are gravitationally bound and resist cosmic expansion. Despite the expansion of intergalactic space, matured galaxies maintain their relatively stable size primarily through gravitational attraction, counterbalanced by the rotational motion of the matter within them. Consequently, each galaxy has a stable local scale

 $\hat{a}$  that remains relatively constant over time, despite increases in the global scale a.

As discussed in Section IIIB, the dilaton field  $\chi$  in intergalactic space is inversely proportional to the global scale factor a. Similarly, within a galaxy, the dilaton field is inversely proportional to the galaxy's local scale  $\hat{a}$ . Since a grows over time whereas  $\hat{a}$  remains relatively stable, the dilaton field declines in the intergalactic space while it remains largely unchanged within galaxies.

For simplicity, we model the local scale  $\hat{a}$  as homogeneous within a galaxy, and allow it to merge with the global scale a at the galaxy's boundary. Importantly, the local scale of the Milky Way may differ from the local scale of the galaxy hosting a specific SNeIa being observed. This is because a gravitationally bound galaxy lives on an FLRW cosmic background that is expanding, rather than static. As a result, its local scale  $\hat{a}$  might, in principle, experience modest growth in response to increases in the global scale a. Therefore, it is reasonable to model the local scale  $\hat{a}$  of a galaxy as a universal function (to be determined) of the redshift z of the galaxy, supplemented by a negligible idiosyncratic component.

Consequently, as the dilaton field  $\chi$  varies across the boundaries of galaxies, the speed of light also varies at the boundaries due to the relationship  $c \propto \chi^{1/2}$ . Figures 1 depicts an intuitive schematic of a lightwave emitted from an SNeIa as it propagates to the Earth-based observer. On its journey, the lightwave undergoes 3 transits:

\* Transit #1: The lightwave emitted from an SNeIa residing "inside host galaxy", which is gravitationally bound and characterized by a local scale  $\hat{a}_{em}$ , must first

exit into the surrounding intergalactic space, characterized by a global scale  $a_{em}$ .

- \* Transit #2: The lightwave then traverses the null geodesic of the FLRW metric and expands along with the cosmic scale factor a(t) of the intergalactic space until it reaches the outskirts of the Milky Way, where the global scale is  $a_{ob}$ .
- \* Transit #3: The lightwave enters the Milky Way, which is gravitationally bound and characterized by a local scale  $\hat{a}_{ob}$ , and finally reaches the Earth-based astronomer's telescope.

While the middle stage of this journey, Transit #2, is well understood in standard cosmology, the first and last stages have been overlooked in previous VSL studies, seriously undermining their analyses and conclusions. In the context of VSL, these stages are crucial due to the additional refraction effects that occur at the boundaries of the host galaxy and the Milky Way.

Figure 2 illustrates the typical behavior of  $\chi^{-1}$ , c, and the wavelength  $\lambda$  along a lightwave trajectory. In the top panel, it can be expected that  $a_{em} > \hat{a}_{em}$  (since the host galaxy resists cosmic expansion),  $a_{ob} > a_{em}$  (due to the expansion of intergalactic space), and  $\hat{a}_{ob} < a_{ob}$  (since the Milky Way also resists cosmic expansion). Quantitatively, we can deduce the variation of wavelength during the three transits as follows:

- The emission event: an SNeIa radiates a wavetrain with a specific wavelength  $\hat{\lambda}_{em}$ .
- Transit #1: The wavetrain exits the host galaxy to enter the surrounding intergalactic space. During this transition, its wavelength is compressed to  $\lambda_{em}$  due to the reduction in the speed of light from  $\hat{c}_{em}$  to  $c_{em}$  across the host galaxy's boundary, viz.

$$\frac{\lambda_{em}}{\hat{\lambda}_{em}} = \frac{c_{em}}{\hat{c}_{em}} = \frac{a_{em}^{-1/2}}{\hat{a}_{em}^{-1/2}} \tag{28}$$

Appendix A summarizes the components involved in the refraction that is induced by variations in the velocity of wavetrains.

• Transit #2: The wavetrain follows the null geodesics of the FLRW metric. As it approaches the outskirts of the Milky Way, its wavelength has expanded from  $\lambda_{em}$  to  $\lambda_{ob}$ , as given in Eq. (26), viz.

$$\frac{\lambda_{ob}}{\lambda_{em}} = \frac{a_{ob}}{a_{em}} \qquad \text{(see Eq. (26))}$$

• Transit #3: The wavetrain enters the Milky Way and reaches the astronomer's telescope. Its wavelength is further prolonged due to an increase in the speed of light from  $c_{ob}$  to  $\hat{c}_{ob}$  across the Milky

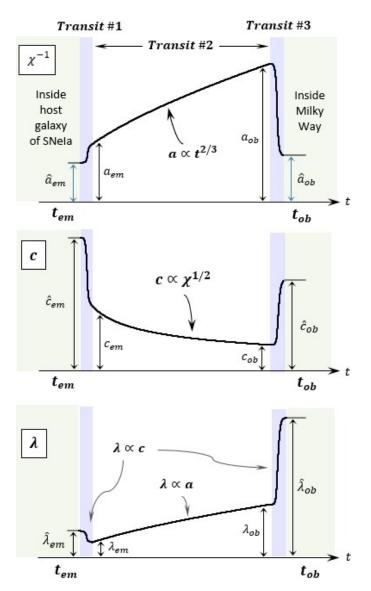


Figure 2. Variations of inverse dilaton (upper panel), speed of light (middle panel), and wavelength (lower panel) along the lightwave trajectory from emission to observation.

Way's boundary, viz.

$$\frac{\hat{\lambda}_{ob}}{\lambda_{ob}} = \frac{\hat{c}_{ob}}{c_{ob}} = \frac{\hat{a}_{ob}^{-1/2}}{a_{ob}^{-1/2}}.$$
 (29)

## C. The "benchmark" wavelength

There is one more crucial element to consider. In calculating the redshift of an SNeIa, it would be *incorrect* to directly compare the observed wavelength  $\hat{\lambda}_{ob}$  with the emitted wavelength  $\hat{\lambda}_{em}$ . This is because  $\hat{\lambda}_{em}$  is associated with the emission event occurring inside the host galaxy, and the observer cannot directly measure  $\hat{\lambda}_{em}$  since she is located within the Milky Way. If the SNeIa

were situated inside the Milky Way, it would emit a wavelength  $\lambda^*$  that differs from  $\hat{\lambda}_{em}$ , as the two galaxies can have different values of local scales,  $\hat{a}_{em}$  versus  $\hat{a}_{ob}$ . The wavelength  $\lambda^*$ , which the observer can measure, is the "benchmark" wavelength to be compared with the observed  $\hat{\lambda}_{ob}$  in calculating the redshift.

To illustrate this issue, let us recall that the lengthscale of any physical process is inversely proportional to the dilaton field, according to Eq. (13) in Section II. For a galaxy, the dilaton field is in turn inversely proportional to the local scale of that galaxy. Consider two identical atoms, one located inside the host galaxy and the other within the Milky Way. If the atom in the host galaxy emits a lightwave with wavelength  $\hat{\lambda}_{em}$ , its counterpart in the Milky Way emits an *identical* lightwave but with wavelength  $\lambda^*$  adjusted to the Milky Way's local scale. The following equality holds

$$\frac{\lambda^*}{\hat{\lambda}_{em}} = \frac{\hat{a}_{ob}}{\hat{a}_{em}} \tag{30}$$

As shown in the right side of Figure 1, the observer must compare  $\hat{\lambda}_{ob}$  with her "benchmark" wavelength  $\lambda^*$ . Finally, the observer calculates the redshift z as the relative change between the observed wavelength and the "benchmark" wavelength, given by

$$z := \frac{\hat{\lambda}_{ob} - \lambda^*}{\lambda^*} \,. \tag{31}$$

We should note that allowing  $\hat{a}_{ob}$  to differ from  $\hat{a}_{em}$  creates a potential pathway to resolving the  $H_0$  tension, a topic that will be discussed in Section X.

# V. MODIFYING REDSHIFT FORMULAE AND HUBBLE LAW USING VARYING C

We are now fully equipped to derive cosmographic formulae applicable to our VSL cosmology.

## A. Modifying the Lemaître redshift formula

What is remarkable in the demonstration depicted in Figure 1 is that the stretching of the wavecrest during Transit #3 does *not* cancel out the compression of the wavecrest during Transit #1. The net effect of the two transits increases the value of z and results in a new formula for the redshift. Below is our derivation.

Combining Eq. (31) with Eqs. (28), (26), and (29), we obtain

$$1 + z = \frac{\hat{\lambda}_{ob}}{\lambda^*} = \frac{\hat{\lambda}_{ob}}{\lambda_{ob}} \cdot \frac{\lambda_{ob}}{\lambda_{em}} \cdot \frac{\lambda_{em}}{\hat{\lambda}_{em}} \cdot \frac{\hat{\lambda}_{em}}{\lambda^*} = \frac{a_{ob}^{3/2}}{a_{em}^{3/2}} \cdot \frac{\hat{a}_{ob}^{3/2}}{\hat{a}_{ob}^{3/2}}$$
(32)

Defining the ratio of local scales as a function of redshift:

$$\frac{\hat{a}_{em}}{\hat{a}_{ob}} := F(z) \tag{33}$$

where F(z=0)=1, and setting

$$a := \frac{a_{em}}{a_{ob}} \tag{34}$$

we arrive at the modified Lemaître redshift formula:

$$1 + z = a^{-3/2} F^{3/2}(z) (35)$$

If  $F(z) \equiv 1 \,\forall z$ , viz. all galaxies have the same local scale, the modified Lemaître redshift formula simplifies to:

$$1 + z = a^{-3/2} (36)$$

These formulae are decisively different from the classic Lemaître redshift formula,  $1 + z = a^{-1}$ . The 3/2–exponent in the modified Lemaître formulae arises as a result of the anisotropic time scaling in Eq. (15).

It is essential to emphasize that the alteration in wavelength—due to the refraction effect across boundaries of galaxies—is instrumental in enabling the VSL effects to manifest in the modified Lemaître redshift formula. To the best of our knowledge, existing VSL analyses in the literature have not considered this wavelength alteration. This omission hinders theirs ability to detect the effects of VSL on the Hubble diagram of SNeIa and late-time cosmic acceleration.

# B. Modifying the Hubble law: An emergent multiplicative factor of 3/2

The current-time Hubble constant  $H_0$  is defined as

$$H_0 := \frac{1}{a} \frac{da}{dt} |_{t=t_0} \tag{37}$$

For a low-z emission source, this yields

$$a = 1 + H_0(t - t_0) + \dots$$
 (38)

Let  $d=c_0.(t_0-t)$  represent the distance from Earth to the emission source, and note that  $F(z)\simeq 1$  for low z. For small z and d, the Taylor expansion for the modified Lemaî redshift formula obtained in Eq. (35) produces the modified Hubble law:

$$z = \frac{3}{2}H_0 \frac{d}{c_0} \tag{39}$$

In comparison to the classic Hubble law, where the speed of light is explicitly restored:

$$z_{\text{(classic)}} = H_0 \frac{d}{c} \tag{40}$$

the modified Hubble law acquires a multiplicative prefactor of 3/2. A significant consequence of this adjustment is a (re)-evaluation of the Hubble constant  $H_0$ , which has implications for BDRS's CMB analysis and the age problem—topics that will be discussed in Sections VIII and IX.

## C. Modifying the distance-redshift formula

Using the evolution  $a \propto t^{2/3}$  per Eq. (17), we can derive that

$$H(t) = \frac{1}{a}\frac{da}{dt} = \frac{2}{3t} = H_0 a^{-3/2}$$
 (41)

The modified Lemaître redshift formula, Eq. (35), can be recast as

$$\ln\frac{(1+z)^{2/3}}{F} = -\ln a \tag{42}$$

and, with the aid of Eq. (41), renders

$$d\ln\frac{(1+z)^{2/3}}{F} = -H_0 a^{-3/2} dt \tag{43}$$

For the modified FLRW metric described in Eq. (20), the coordinate distance in flat space is

$$r = c_0 \int_{t_{em}}^{t_{ob}} \frac{dt}{a^{3/2}(t)} \tag{44}$$

From Eqs. (43) and (44), and noting that F(z=0)=1, we obtain the *modified* distance–redshift formula in a compact expression

$$\frac{r}{c_0} = \frac{1}{H_0} \ln \frac{(1+z)^{2/3}}{F} \,. \tag{45}$$

# D. Modifying the luminosity distance–redshift formula

In standard cosmology, the luminosity distance  $d_L$  is defined via the absolute luminosity L and the apparent luminosity J:

$$d_L^2 = \frac{L}{4\pi J} \tag{46}$$

The absolute luminosity L and the apparent luminosity J are related as

$$4\pi r^2 J = L \frac{\hat{\lambda}_{em}}{\hat{\lambda}_{ob}} \cdot \frac{\hat{\lambda}_{em}}{\hat{\lambda}_{ob}} \tag{47}$$

In the right hand side of Eq. (47), the first term  $\hat{\lambda}_{em}/\hat{\lambda}_{ob}$  represents the "loss" in energy of the redshifted photon known as the "Doppler theft" <sup>2</sup>. The second (identical) term  $\hat{\lambda}_{em}/\hat{\lambda}_{ob}$  arises from the dilution factor in photon

density, as the same number of photons is distributed over a prolonged wavecrest in the radial direction (i.e., along the light ray). The  $4\pi r^2$  in the left hand side of Eq. (47) accounts for the spherical dilution in flat space. From (46) and (47), we obtain

$$d_L = r \frac{\hat{\lambda}_{ob}}{\hat{\lambda}_{em}} \tag{48}$$

Using the definitions of redshift and the "benchmark" wavelength, Eqs. (31) and (30) respectively, the luminosity distance becomes

$$d_L = r \frac{\hat{\lambda}_{ob}}{\lambda^*} \cdot \frac{\lambda^*}{\hat{\lambda}_{em}} = r (1+z) \frac{\hat{a}_{ob}}{\hat{a}_{em}}$$
(49)

or, by including (33):

$$d_{L} = r(1+z)\frac{1}{F(z)}$$
 (50)

Due to the refraction effect during Transit #3, the apparent luminosity distance observed by the Earth-based astronomer  $\hat{d}_L$  differs from  $d_L$  by the factor  $\hat{c}_{ob}/c_{ob}$ , viz.

$$\frac{\hat{d}_L}{\hat{c}_{ob}} = \frac{d_L}{c_{ob}} \tag{51}$$

Finally, combining Eqs. (45), (50), and (51), we arrive at the *modified* luminosity distance–redshift relation:

$$\frac{\hat{d}_L}{\hat{c}_{ob}} = \frac{1+z}{H_0 F(z)} \ln \frac{(1+z)^{2/3}}{F(z)}$$
 (52)

where  $\hat{d}_L$  is the luminosity distance observed by the Earth-based astronomer and  $\hat{c}_{ob}$  the speed of light measured in the Milky Way (i.e., 300,000 km/s). Formula (52) contains a single parameters  $H_0$  and involves a function F(z) that captures the evolution of the local scale of galaxies as a function of redshift.

# VI. RE-ANALYZING PANTHEON CATALOG USING VARYING C

This section applies the new formula, Eq. (52), to the Combined Pantheon Sample of SNeIa. In [95], Scolnic and collaborators produced a dataset of apparent magnitudes for 1,048 SNeIa with redshift z ranging from 0.01 to 2.25, accessible in [96]. For each SNeIa  $i^{th}$ , the catalog provides the redshift  $z_i$ , the apparent magnitude  $m_{B,i}^{\text{Pantheon}}$  together with its error bar  $\sigma_i^{\text{Pantheon}}$ . We apply the absolute magnitude M=-19.35 to compute the distance modulus,  $\mu^{\text{Pantheon}}:=m_B^{\text{Pantheon}}-M$ . The distance modulus is then converted to the luminosity distance  $d_L$  using the following relation:

$$\mu = 5 \log_{10}(d_L/\text{Mpc}) + 25$$
 (53)

The Pantheon data, along with their error bars, are displayed in the Hubble diagram shown in Fig. 3.

 $<sup>^2</sup>$  Note: This energy loss is consistent with the scaling property of energy for our VSL mechanism, as described by Eq. (13) in Section II. In intergalactic space, the energy of the traveling photon scales as  $E \propto \chi \propto a^{-1}$ , leading to a decline in energy as the universe expands.

# A. $\Lambda$ CDM and standard EdS as benchmarking models

For benchmarking purposes, we first fit the Pantheon Catalog with the flat  $\Lambda$ CDM model. The luminosity distance–redshift relation for this model is a well-established result (where  $\Omega_M + \Omega_{\Lambda} = 1$ )

$$\frac{d_L}{c} = \frac{1+z}{H_0} \int_0^z \frac{dz'}{\sqrt{\Omega_M (1+z')^3 + \Omega_\Lambda}}$$
 (54)

Our fit will minimize the normalized error

$$\chi^2 := \frac{1}{N} \sum_{j=1}^{N} \left( \frac{\mu_j^{\text{model}} - \mu_j^{\text{Pantheon}}}{\sigma_j^{\text{Pantheon}}} \right)^2 \tag{55}$$

with the sum taken over all N=1,048 Pantheon data points. The best fit for the  $\Lambda \text{CDM}$  model yields  $H_0=70.2 \text{ km/s/Mpc}$ ,  $\Omega_M=0.285$ ,  $\Omega_{\Lambda}=0.715$ , with the minimum error  $\chi^2_{\min}(\Lambda \text{CDM})=0.98824$ . The  $d_L$ –z curve for the  $\Lambda \text{CDM}$  model is depicted by the dashed line in Fig. 3.

Also for benchmarking purposes, we consider a "fiducial" model: the standard EdS universe (i.e. with constant speed of light). The luminosity distance—redshift formula for this fiducial model can be obtained by setting  $\Omega_{\Lambda} = 0$  and  $\Omega_{M} = 1$  in Eq. (54), yielding

$$\frac{d_L}{c} = 2\frac{1+z}{H_0} \left( 1 - \frac{1}{\sqrt{1+z}} \right) \tag{56}$$

Figure 3 displays the  $d_l$ –z curve as a dotted line for the fiducial EdS model (using the  $H_0=70.2$  value obtained above for the  $\Lambda {\rm CDM}$  model). This curve fits well with the Pantheon data for low z but fails to capture the data for high z. The Pantheon data with  $z\gtrsim 0.1$  show an excess in the distance modulus compared with the baseline EdS model, meaning that high-redshift SNeIa appear dimmer than predicted by the fiducial EdS model. As a result, this discrepancy necessitated the introduction of the  $\Lambda$  component, commonly referred to as dark energy, characterized by an equation of state w=-1 and an energy density of  $\Omega_{\Lambda}\approx 0.7$ .

#### B. Fitting with VSL model: Disabling F(z)

In this subsection, we will disable the evolution of the local scale of galaxies by setting  $F(z) \equiv 1$  in Formula (52). This means that the fit is carried out with respect to a simplified formula with one adjustable parameter  $H_0$ :

$$\frac{\hat{d}_L}{\hat{c}_{ob}} = \frac{1+z}{\frac{3}{2}H_0} \ln(1+z) \tag{57}$$

Hereafter, the luminosity distance  $\hat{d}_L$  observed by the Earth-based astronomer will be used in the conversion described by Eq. (53).

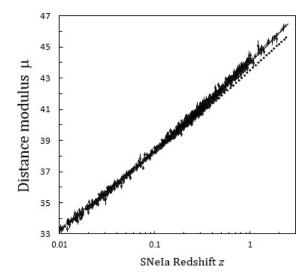


Figure 3. Fitting Pantheon using Formula (57). Open circles: 1,048 data points with error bars. Solid line: our Formula (57) with  $H_0=44.4$ . Dashed line:  $\Lambda \text{CDM}$  Formula (54) with  $H_0=70.2$ ,  $\Omega_{\Lambda}=0.715$ . Dotted line: EdS Formula (56) with  $H_0=70.2$ .

The best fit of the Pantheon data to this formula yields  $H_0 = 44.4 \text{ km/s/Mpc}$ , corresponding to  $\chi^2_{\min} = 1.25366$ . Figure 3 displays our fit as the solid line. Although this fit performs worse than the  $\Lambda\text{CDM}$  model, which has  $\chi^2_{\min}(\Lambda\text{CDM}) = 0.98824$ , it substantially reduces the excess in distance moduli for  $z \gtrsim 0.1$  compared with the "fiducial" EdS model, as shown in Fig. 3.

We must emphasize that both Formulae (56) and (57) are one-parameter models. Both models are based on an EdS universe, but our VSL model accommodates varying speed of light, whereas the "fiducial" EdS model operates under the assumption of a constant speed of light. Therefore, we can conclude that varying speed of light is responsible for the improved performance of our VSL model compared to the "fiducial" EdS model.

This aspect can be explained as follows. In the high z limit, Formula (56) of the "fiducial" EdS model yields

$$d_L \simeq z \tag{58}$$

whereas Formula (57) of our VSL model gives

$$d_L \propto \hat{d}_L \simeq z \, \ln z \tag{59}$$

The additional  $\ln z$  term in Eq. (59) compared to Eq. (58) induces a steeper slope in the high–z portion of the  $d_L$ –z curve, which translates to an excess in distance modulus at high redshift. Notably, our VSL model does not require dark energy whatsoever to account for this behavior.

The performance of our VSL model can be improved by enabling the function F(z), which involves allowing the local scales of galaxies to evolve. This task will be carried out in the following subsections.

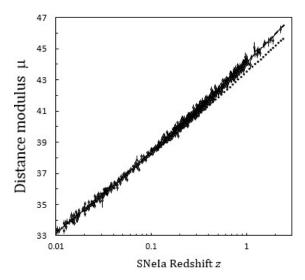


Figure 4. Fitting Pantheon using Formula (60). Open circles: 1,048 data points with error bars. Solid line: our Formula (60) with  $H_0=46.6$  and the  $F^{(i)}$  values given in Table I. Dashed line:  $\Lambda$ CDM Formula (54) with  $H_0=70.2$ ,  $\Omega_{\Lambda}=0.715$ . Dotted line: EdS Formula (56) with  $H_0=70.2$ .

Bin	Number of SNeIa	$\min z$	$\operatorname{Max} z$	$F^{(i)}$
#1	105	0.010	0.032	1.000
#2	105	0.032	0.096	1.000
#3	105	0.099	0.159	0.997
#4	105	0.159	0.203	0.996
#5	105	0.203	0.249	0.994
#6	105	0.249	0.299	0.994
#7	105	0.300	0.366	0.988
#8	105	0.368	0.508	0.984
#9	105	0.510	0.742	0.978
#10	103	0.743	2.260	0.968

Table I. Values of  $F^{(i)}$  for the 10 respective bins.

### C. Enabling F(z): A binning approach

In this subsection, we will incorporate the variation in the local scales of galaxies, as characterized by F(z). Developing model for F(z) would require knowledge of galactic formation and structures. Here, we avoid that complexity by extracting F(z) directly from the Pantheon data. To do so, we spit the Pantheon dataset into 10 bins ordered by increasing redshift. Bins #1 to #9 each contains 105 data points, while Bin #10 contains 103 data points, totaling 1,048 data points. The range of redshift for each bin is given in Table I.

All Pantheon data points in Bin #i are treated as having a common value of  $F^{(i)}$  for the function F(z). For a data point #j that belongs to Bin #i, Formula (52) reads

$$\frac{\hat{d}_{L,j}}{\hat{c}_{ob}} = \frac{1+z_j}{H_0 F^{(i)}} \ln \frac{(1+z_j)^{2/3}}{F^{(i)}}$$
 (60)

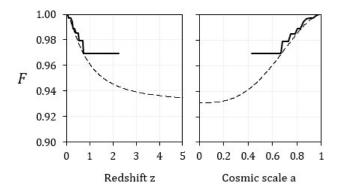


Figure 5. The variation of F(z) as functions of redshift (left panel) and cosmic scale factor (right panel). Solid staircase lines are the result obtained in Section VIC. Dashed lines are the result obtained in Section VID.

Instead of fitting each bin separately, we impose one common value for  $H_0$  across all bins. The fit thus involves  $H_0$  and 10 values for  $\{F^{(i)}, i=1..10\}$ . Figure 4 displays our fit to Formula (60). The best fit yields  $H_0=46.6$  km/s/Mpc, and the values of  $F^{(i)}$  are given in the last column of Table I. The minimum error is  $\chi^2_{\min}=0.97803$ . The staircase lines in Fig. 5 depict  $F^{(i)}$  as function of z and the cosmic factor a.

The values  $F^{(i)}$  reveal a monotonic decrease with respect to redshift, or equivalently, a monotonic increase in terms of a. This behavior indicates that the local scales of galaxies gradually grow during the course of cosmic expansion, implying that galaxies cannot fully resist this expansion. From  $z \simeq 2$  to the present time, galaxies have slightly expanded by about 3%, during which process the cosmic scale factor has approximately doubled, i.e.  $a|_{z\simeq 2}\simeq 0.5$  with  $F(z\simeq 2)\approx 0.969$ .

#### D. Enabling F(z): A parametrization approach

The steady decline of  $F^{(i)}$  across the 10 bins with respect to redshift suggests adopting the following parametrization for F(z):

$$F(z) = 1 - (1 - F_{\infty}) \left( 1 - (1 + z)^{-b_1} \right)^{b_2}$$
 (61)

with  $b_1 \in \mathbb{R}^+$ ,  $b_2 \in \mathbb{R}^+$ , and  $F_{\infty} \in [0,1]$ , supporting a monotonic interpolation from F(z=0)=1 to  $F(z \to \infty)=F_{\infty}$ . After some experimentation, we find that setting  $b_1=b_2=2$  offers good overall performance.

We will apply Formula (52) in conjunction with (61) (with  $b_1 = b_2 = 2$ ) to fit the Pantheon dataset. The best fit is displayed in Fig. 6, yielding  $H_0 = 47.22$  and  $F_{\infty} = 0.931$ . The minimum error is  $\chi^2_{\min} = 0.98556$ , a performance that is competitive with—if not exceeding—that of the  $\Lambda$ CDM model, which has  $\chi^2_{\min}(\Lambda$ CDM) = 0.98824.

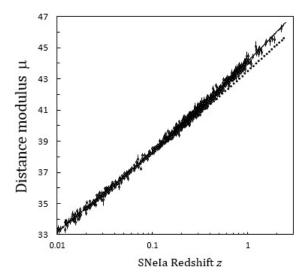


Figure 6. Fitting Pantheon using Formula (52). Open circles: 1,048 data points with error bars. Solid line: our Formula (52) with  $H_0=47.22$ , and F(z) given in Eq. (61) with  $b_1=b_2=2$  and  $F_{\infty}=0.931$ . Dashed line:  $\Lambda$ CDM Formula (54) with  $H_0=70.2$ ,  $\Omega_{\Lambda}=0.715$ . Dotted line: EdS Formula (56) with  $H_0=70.2$ .

Figure 5 shows the variation of F in dashed lines with respect to both redshift and the cosmic factor. We also produce the joint distribution for  $H_0$  and  $F_{\infty}$ , as shown in Figure 7, yielding  $H_0 = 47.21 \pm 0.4$  km/s/Mpc (95% CL) and  $F_{\infty} = 0.931 \pm 0.008$  (95% CL). This value of  $F_{\infty}$  indicates that the local scales of galaxies have increased by approximately 7% since the formation of the first stable galaxies (i.e., those at the largest redshift).

# Comparison of VSL approach with $\Lambda$ CDM model

Our VSL fit, in effect, involves two parameters:  $H_0$  and  $F_{\infty}$ —the same number of parameters as the  $\Lambda$ CDM model ( $H_0$  and  $\Omega_{\Lambda}$ ). However, the parameter  $F_{\infty}$  has a well-defined astrophysical meaning; it denotes the local scales of the first stable galaxies in comparison to the local scale of the Milky Way. Moreover, the function F(z), which captures the evolution of the local scales of galaxies during cosmic expansion, plays a role in a potential resolution of the  $H_0$  tension—a topic that will be discussed in Section X.

In contrast, the  $\Lambda$ CDM model requires a  $\Lambda$  component, the nature of which is still not understood. Its energy density value  $\Omega_{\Lambda} \approx 0.7$  also raises a coincidence problem. Furthermore, the  $\Lambda$ CDM model currently encounters the  $H_0$  tension. If the  $\Lambda$  component is treated as dynamical—an approach explored in several ongoing efforts to resolve the  $H_0$  tension—this would introduce an array of new parameters to the  $\Lambda$ CDM model.

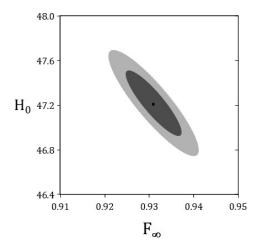


Figure 7. Joint distribution of  $H_0$  and  $F_{\infty}$ , showing 68% CL and 95% CL regions. Peak occurs at  $H_0 = 47.22$ ,  $F_{\infty} = 0.931$ .

## E. The cause for the reduction in $H_0$ value

In the  $z \to 0$  limit, Eq. (61) with  $b_1 = b_2 = 2$  can be approximated as

$$F(z) \simeq 1 - 4(1 - F_{\infty}) z^2 + \dots$$
 (62)

From this, Formula (52) then gives

$$\frac{\hat{d}_L}{\hat{c}_{ch}} = \frac{2}{3H_0} z + \mathcal{O}(z^2) \tag{63}$$

leading to the modified Hubble law:

$$z = \frac{3}{2}H_0 \frac{\hat{d}_L}{\hat{c}_{ob}} \tag{64}$$

This result aligns with Eq. (39) derived in Section VB based on the modified Lemaître redshift formula, Eq. (35). In contrast to the classic Hubble law, where the speed of light is constant:

$$z_{\text{(classic)}} = H_0 \frac{d_L}{c}$$
 (see Eq. (40))

the modified Hubble law acquires a multiplicative factor of 3/2. Hence, in our VSL cosmology, low-redshift emission sources exhibit a linear relationship between z and the luminosity distance, but characterized by a coefficient of  $\frac{3}{2}H_0$  rather than  $H_0$ .

Since a linear-line fit of z on  $d_L$  for low-redshift emission sources is known to yield a slope of approximately 70, the resulting value of  $H_0$  obtained through our VSL approach is thus only 2/3 of this value, specifically  $H_0 \approx 47$ , rather than  $H_0 \approx 70$  as predicted by standard cosmology.

# VII. A NEW INTERPRETATION: VARIABLE SPEED OF LIGHT AS AN ALTERNATIVE TO DARK ENERGY AND COSMIC ACCELERATION

The Hubble diagram of SNeIa has been interpreted as a definitive hallmark of late-time accelerated expansion, providing the (only) direct evidence for dark energy. These stellar explosions serve as "standard candles" due to their consistent peak brightness, allowing astronomers to determine distances to the galaxies in which they reside. In the late 1990s, two independent teams, the High-Z Supernova Search Team [97] and the Supernova Cosmology Project [98], measured the apparent brightness of distant SNeIa, finding them dimmer than expected based on the EdS model, which describes a flat, expanding universe dominated by matter. This can be seen in the Hubble diagram of SNeIa (see Fig. (4)), in which the section with  $z \gtrsim 0.1$  exhibits an distance modulus greater than that predicted by the EdS model. This behavior has been interpreted as indicating that the expansion of the universe is accelerating rather than decelerating.

However, our quantitative analysis of SNeIa in the preceding section offers a new interpretation as an alternative to late-time acceleration. Mathematically, as explained in Section VIB, in the high z limit, the EdS universe yields

$$d_L \simeq z$$
 (see Eq. (58))

whereas our VSL-based formula renders

$$d_L \simeq z \ln z$$
 (see Eq. (59))

Thus, high-redshift SNeIa acquire an additional factor of  $\ln z$  compared with the EdS model. This results in an further upward slope relative to that of the EdS model, successfully capturing the behavior of SNeIa in the high-z section.

**Physical intuition:** There is a fundamental reason based on our VSL framework—behind this excess in distance modulus that we will explain below. Consider two supernovae A and B at distances  $d_A$  and  $d_B$  away from the Earth, such that  $d_B = 2 d_A$ . In standard cosmology, their redshift values  $z_A$  and  $z_B$  are related by  $z_A \approx 2 z_A$ (to first-order approximation). However, this relation breaks down in the VSL context. In a VSL cosmology which accommodates variation in the speed of light in the formize  $c \propto a^{-1/2}$ , light traveled faster in the distant past (when the cosmic factor  $a \ll 1$ ) than in the more recent epoch (when  $a \lesssim 1$ ). Therefore, the photon emitted from supernova B was able to cover twice the distance in less than twice the time required for the photon emitted from supernova A. Having spent less time in transit than what standard cosmology would require, the B-photon experienced less cosmic expansion than expected and thus a lower redshift than what the classic Lemaître formula would dictate. Namely:

$$z_B < 2 z_A \quad \text{for } d_B = 2 d_A \tag{65}$$

Conversely, consider a supernova C with  $z_C = 2\,z_A$ . For the C-photon to experience twice the redshift of the A-photon, it must travel a distance greater than twice that of the A-photon, viz.:  $d_C > 2\,d_A$ . This is because since the C-photon traveled faster at the beginning of its journey toward Earth, it must originate from a farther distance (thus appearing fainter than expected) to experience enough cosmic expansion and therefore the requisite amount of redshift. Namely:

$$d_C > 2 d_A \quad \text{for} \quad z_C = 2 z_A \tag{66}$$

Consequently, the SNeIa data exhibit an additional upward slope in their Hubble diagram in the high-z section.

Conclusion: Hence, a declining speed of light presents a viable alternative to cosmic acceleration, eliminating the need for the  $\Lambda$  component and dissolving its finetuning and coincidence problems. In our VSL framework, during the universe expansion, the dilaton field  $\chi$  in intergalactic space decreases and leads to a decline in c (per  $c \propto \chi^{1/2} \propto a^{-1/2}$ ), affecting the propagation of lightwaves from distant SNeIa to the observer. While the impact of a declining c on lightwaves is negligible within the Solar System and on galactic scales, it accumulates on the cosmic scale and makes high-redshift SNeIa appear dimmer than predicted by the standard EdS model.

The VSL framework, therefore, offers a significant shift in perspective: rather than supporting a  $\Lambda CDM$  universe undergoing late-time acceleration, the Hubble diagram of SNeIa should be reinterpreted as evidence for a declining speed of light in an expanding Einstein-de Sitter universe.

# VIII. RETHINKING BLANCHARD-DOUSPIS-ROWAN-ROBINSON-SARKAR'S 2003 CMB ANALYSIS AND $H_0 \approx 46$

Let us now turn our discussion to a remarkable proposal advanced by Blanchard, Douspis, Rowan-Robinson, and Sarkar (BDRS) in 2003 and its relation to our SNeIa analysis.

It is well established that the  $\Lambda$ CDM model, augmented by the primordial fluctuation spectrum (presumably arising from inflation) in the form  $P(k) = A \, k^n$ , successfully accounts for the observed anisotropies in the cosmic microwave background (CMB). This model predicts a dark energy density of  $\Omega_{\Lambda} \approx 0.7$ , a Hubble constant of  $H_0 \approx 67$ , and a spectral index  $n \approx 0.96$  [99, 100]. Yet, in [4] BDRS reanalyzed the CMB, available at the time from the Wilkinson Microwave Anisotropy Probe (WMAP), in a new perspective. These authors deliberately relied on the EdS model, which corresponds to a flat  $\Lambda$ CDM model with  $\Omega_{\Lambda} = 0$ . Rather than invoking the  $\Lambda$  component, they adopted a slightly modified form for the primordial fluctuation spectrum. They reasoned that, since the spectral index n is scale-dependent for

any polynomial potential of the inflaton and is constant only for an exponential potential, it is reasonable to consider a double-power form for the spectrum of primordial fluctuations

$$P(k) = \begin{cases} A_1 k^{n_1} & k \leq k_* \\ A_2 k^{n_2} & k \geqslant k_* \end{cases}$$
 (67)

with a continuity condition  $(A_1 k_*^{n_1} = A_2 k_*^{n_2})$  across the breakpoint  $k_*$ .

Using this new function, BDRS produced an excellent fit to the CMB power spectrum, resulting in the following parameters:  $H_0 = 46 \text{ km/s/Mpc}$ ,  $\omega_{\text{baryon}} := \Omega_{\text{baryon}}(H_0/100)^2 = 0.019$ ,  $\tau = 0.16$  (the optical depth to last scattering),  $k_* = 0.0096 \text{ Mpc}^{-1}$ ,  $n_1 = 1.015$ , and  $n_2 = 0.806$ . The most remarkable outcome of the BDRS work is the "low" value of  $H_0 = 46$ , representing a 34% reduction from the accepted value of  $H_0 \sim 70$ . A detailed follow-up study by Hunt and Sarkar [5], based on a supergravity-induced multiple inflation scenario, yielded a comparable value of  $H_0 \approx 44$ . Notably, around the same time, Shanks argued that a value of  $H_0 \lesssim 50$  might permit a simpler inflationary model with  $\Omega_{\text{baryon}} = 1$ , i.e. without invoking dark energy or cold dark matter [101].

The success achieved by BDRS in reproducing the CMB power spectrum can be interpreted as indicating a degeneracy in the parameter space  $\{\Omega_{\Lambda}, H_0\}$ . Specifically, the BDRS pair  $\{\Omega_{\Lambda}=0, H_0=46\}$  is 'nearly degenerate' with the canonical pair  $\{\Omega_{\Lambda}\approx 0.7, H_0\approx 70\}$ , insofar as the CMB data is concerned. Importantly, BDRS's modest modification in the primordial fluctuation spectrum can make  $\Omega_{\Lambda}$  redundant. In other words, the  $\Lambda$  component is vulnerable to other exogenous underlying assumptions that supplement the  $\Lambda$ CDM model.

Notably, strong degeneracies in the parameter space related to the CMB have been reported recently. In [102] Alestas et al found that the best-fit value of  $H_0$  obtained from the CMB power spectrum is degenerate with a constant equation of state (EoS) parameter w; the relationship is approximately linear, given by  $H_0 + 30.93\,w - 36.47 = 0$  (with  $H_0$  in km/s/Mpc). Although this finding is not directly related to the BDRS work, the  $H_0$ -vs-w degeneracy reinforces the general conclusion regarding the sensitivity of  $H_0$  to other exogenous underlying assumptions that supplement the  $\Lambda$ CDM model—in the case of Alestas et al, the EoS parameter w.

While a drastically low value of  $H_0 \approx 46$  at first seems to be 'a steep price to pay', we have demonstrated in the preceding sections that this new value is fully compatible with the  $H_0 = 47.2$  obtained from the Hubble diagram of SNeIa data when analyzed within the context of VSL cosmology. Consequently, the  $\Lambda$  component becomes redundant not only for the CMB but also for SNeIa.

The alignment of our findings with those of BDRS is especially remarkable for several reasons:

- The Hubble diagram of SNeIa and the CMB power spectrum are two "orthogonal" datasets. SNeIa data relates to observations along the time direction, while the CMB captures a two-dimensional snapshot across space at the recombination event. Furthermore, they correspond to two separate epochs—one representing late time (SNeIa) and the other representing early time (CMB)— each characterized by distinct relevant physics.
- There is no a priori reason to expect the double-power primordial fluctuation spectrum used in the BDRS work to result in a reduction in  $H_0$  rather than an enhancement. Moreover, there is no inherent indication of the 34% change in  $H_0$ . The strength of our VSL analysis of SNeIa is in its capability to explain both the direction and magnitude of the change in  $H_0$  through the 3/2-factor in the modified Hubble law; see Section VI E.
- Our VSL framework is inspired from theoretical consideration of scale-invariant actions (see Section II herein and Ref. [6]) and does not rely on prior knowledge of BDRS's analysis. It was not deliberately designed to address BDRS's surprise finding of  $H_0 \approx 46$ . In this regard, our findings should be viewed as a retrodiction of BDRS's results, supporting  $H_0 \sim 46$ –47 and bypassing the need for the  $\Lambda$  component.

Together with our SNeIa analysis, the work of BDRS eliminates the need for the  $\Lambda$  component regarding the two 'orthogonal' datasets—the CMB and SNeIa. Future applications of our VSL framework to gravitational lensing, Baryonic Acoustic Oscillations (BAO), and other areas are worthwhile.

# What caused BDRS to abandon their $H_0 \approx 46$ finding?

In 2006 BDRS revisited their 2003 A&A proposal by applying it to the Sloan Digital Sky Survey (SDSS) of luminous red galaxies (LRG) which became available in [103]. In their 2006 follow-up work [104], BDRS claimed that the "low" value of  $H_0 \approx 46$  was unable to produce an acceptable fit to the two-point correlation function of LRG in observed (redshift) space. The upper panel of Fig. 8 reproduces their finding, showing that the SDSS data (and their error bars in red segments) largely aligns with the  $\Lambda$ CDM model (dotted line), while the BDRS model (dashed-dotted line) is significantly off. This discrepancy eventually forced BDRS to abandon their 2003 proposal in its entirety (although Hunt and Sarkar continued with their follow-up study shortly thereafter [5]).

However, we believe that BDRS's 2006 SDSS analysis contained an oversight, in light of our VSL cosmology. The standard Lemaître redshift formula and the conventional Hubble law are not applicable in the presence of

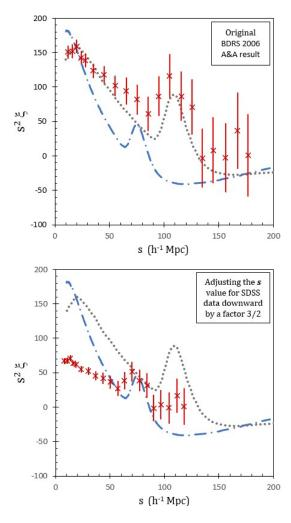


Figure 8. The correlation function in observed (redshift) space, as reproduced from BDRS's 2006 SDSS study [104]. Upper panel: BDRS's original result. Lower panel: the SDSS data are corrected by reducing s and  $s^2 \xi$  by factors of 3/2 and  $(3/2)^2$ , respectively.

varying speed of light. As discussed in Sections V A and V B, these expressions are modified by a factor of 3/2 due to varying c. Therefore, the SDSS would need a reevaluation to incorporate this VSL-induced adjustment. Here, we tentatively make a rudimentary fix: we correct the comoving distance s (measured in multiples of h, defined as  $H_0/(100 \text{ km/s/Mpc})$ ), downward by a factor of 3/2. In the lower panel of Fig. 8, we adjust the SDSS data (and their error bars) by reducing s by a factor of 3/2 and  $s^2 \xi$  by a factor of  $(3/2)^2$ . Upon these adjustments, the peak (at  $s \simeq 75$ ) and trough (at  $s \simeq 60$ ) of the SDSS become aligned with those of the BDRS's model (dashed-dotted line), thereby lessening the discrepancy issue that led to BDRS's abandonment of their original proposal.

We conclude that it was *premature* for BDRS to abandon their 2003 CMB study and the finding of  $H_0$ ,  $\approx 46$ . Rather, their proposal should be revived and applied to

the upgraded Planck dataset for the CMB [99]. We should also note that since the CMB data is a two-dimensional snapshot of the sky at the time at recombination, VSL is not expected to be a dominant player in the CMB. Nevertheless, potential impacts of VSL on the CMB are an interesting avenue for future research.

#### IX. RESOLVING THE AGE PROBLEM

From the definition of the Hubble constant,  $H(t) := \frac{1}{a} \frac{da}{dt}$ , and the evolution,  $a \propto t^{2/3}$ , the age of an EdS universe is related to the current-time  $H_0$  value by

$$t_0^{\rm EdS} = \frac{2}{3H_0} \tag{68}$$

A value of  $H_0 \sim 70$ , would result in an age of 9.3 billion years which would be too short to accommodate the existence of the oldest stars—a paradox commonly referred to as the age problem.

Standard cosmology resolves the age problem by invoking the  $\Lambda$  component which induces an acceleration phase following a deceleration phase. The spatially flat  $\Lambda$ CDM model is known to give the age formula in an analytical form (with  $\Omega_M + \Omega_{\Lambda} = 1$  and  $\Omega_{\Lambda} > 0$ ) [105]

$$t_0^{\Lambda {\rm CDM}} = \frac{2}{3\sqrt{\Omega_{\Lambda}}H_0} \operatorname{arcsinh} \sqrt{\frac{\Omega_{\Lambda}}{\Omega_M}}.$$
 (69)

which restores Eq. (68) when  $\Omega_M \to 1$  and  $\Omega_\Lambda \to 0$ . For positive  $\Omega_\Lambda$ , the age exceeds  $2/(3H_0)$ . With  $H_0 = 70.2$ ,  $\Omega_M = 0.285$ ,  $\Omega_\Lambda = 0.715$ , it yields an age of 13.6 billion years, an accepted figure in standard cosmology.

However, our VSL cosmology naturally overcomes the age problem without invoking the  $\Lambda$  component. The reason is that  $H_0$  is reduced by a factor of 3/2, as detailed in Section VIE. The reduced value  $H_0=47.22\pm0.4$  (95% CL) promptly yields  $t_0=13.82\pm0.11$  billion years (95% CL), consistent with the accepted age value, thereby successfully resolving the age problem.

# X. TOWARD A NEW RESOLUTION OF THE $H_0$ TENSION

Galaxies are gravitationally bound structures, stabilized by gravitational attraction and rotational motion of matter within them. However, they are embedded in a cosmic background that is not static, but rather expanding over time. As such, stable galaxies in principle may adjust to the growth in the scale of the "ambient" intergalactic space surrounding them; viz., their local scales may increase in response to the cosmic expansion. This growth in the local scales of galaxies—if it exists—would be of astronomical nature. To investigate this phenomenon, one could explore the evolution of a spinning disc-shaped distribution of matter (serving as a

simplified model for a galaxy) on an expanding cosmic background within the scale-invariant theory mentioned in Section II, although such an exploration lies beyond the scope of this paper. We should note that recent observational studies have reported evidence of galaxies experiencing growth in size [106, 107].

For our purposes, in Section IV, we have modeled the local scale  $\hat{a}$  of an individual galaxy as a function of its redshift z, supplemented with a negligible idiosyncratic component that randomly varies from one galaxy to another. The function F(z), defined in Eq. (33) as the ratio of the local scale of galaxies at redshift z to the local scale of the Milky Way, captures the evolution of the local scale over cosmic time. In Section VIC, F(z) was empirically extracted from the Pantheon Catalog, with Fig. 5 displaying F(z) as a function of the redshift and of cosmic scale factor, respectively. In accordance with our expectation, the local scale  $\hat{a}$  of galaxies gradually increases in response to the growth of the global cosmic factor a over cosmic time.

# A 'running' $\mathbf{H}_0(z)$

The function F(z) can be absorbed into an "effective" Hubble constant  $H_0(z)$  which depends on redshift z. Specifically, Formula (52) can be rewritten as

$$\frac{\hat{d}_L}{\hat{c}_{ob}} = \frac{1+z}{\frac{3}{2}H_0(z)}\ln(1+z)$$
 (70)

where the newly introduced function  $H_0(z)$  is given by

$$H_0(z) = H_0 F(z) \left( 1 - \frac{3}{2} \frac{\ln F(z)}{\ln(1+z)} \right).$$
 (71)

Formulae (70) and (71) thus allow for a current-time  $H_0(z)$  'running' as a function of the redshift of the data that are used to estimate it. With the function F(z) parametrized in Eq. (61) with  $b_1=b_2=2$  and  $F_\infty=0.931$  as produced in Section VID,  $H_0(z)$  can be computed using Eq. (71), as displayed in Fig. 9. At first,  $H_0(z)$  decreases from 47.2 (at z=0) to 41.5 (at  $z\simeq 2$ ), experiencing a 12% reduction. For  $z\gtrsim 2$ ,  $H_0(z)$  slowly rerises. At  $z\to\infty$ , with  $F_\infty=0.931$  and  $H_0(z=0)=47.22$ , per Eq. (71),  $H_0(z)$  asymptotically approaches  $F_\infty H_0=43.96$ , representing an 7% reduction from  $H_0(z=0)$ .

Two immediate remarks can be made:

- 1. Interestingly, the overall 7% reduction in the  $H_0$  estimate at highest-z SNeIa data is of the comparable magnitude with the discrepancy in  $H_0$  reported in standard cosmology, which observes a decreases of  $H_0$  from 73 (using SNeIa) to 67 (using the Planck CMB), an 8% reduction.
- 2. Remarkably, the asymptotic value  $H_0(z \to \infty) = 43.96$  that we just derived agrees surprisingly well

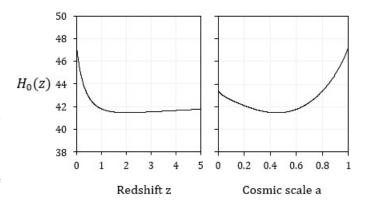


Figure 9. The variation of  $H_0(z)$  as functions of redshift (left panel) and of cosmic scale factor (right panel).

with the  $H_0 \approx 44$  value obtained by Hunt and Sarkar in their follow-up study of the CMB [5].

The 'running' phenomenon of  $H_0(z)$  arises because astronomical objects—either the CMB or SNeIa—are subject to their local scale which gradually grows during the cosmic expansion.

## Hints at an astronomical origin of the H<sub>0</sub> tension

We have, therefore, linked the 'running' current-time  $H_0(z)$  with the function F(z). Since F(z) captures the evolution of galaxies' local scales in response to the growth of the global scale of intergalactic space, the 'running'  $H_0(z)$  is thus of astronomical origin. The empirical evaluation for F(z) from the Pantheon Catalog, as detailed in Sections VIC and VID, demonstrates that the local scale gradually increases with cosmic time, indicating that galaxies cannot fully resist cosmic expansion. As mentioned earlier, understanding the growth in F(z) would require an in-depth examination of a spinning disc-shaped distribution of matter in an expanding cosmic background within a scale-invariant theory of gravity and matter, a task that is left for future investigation.

We should also note similar works along this line of 'running'  $H_0(z)$  [108–110]. For example, in [110], Dainotti et al considered an extension of the flat  $w_0w_aCDM$ . They proposed the following luminosity distance–redshift formula

$$\frac{d_L}{c} = (1+z) \times \int_0^z \frac{dz'}{H_0(z') \sqrt{\Omega_{0M} (1+z')^3 + \Omega_{0\Lambda} e^{3 \int_0^{z'} du \frac{1+w(u)}{1+u}}}}$$
(72)

with the parametrization  $H_0(z) = \tilde{H}_0 (1+z)^{-\alpha}$  and an evolutionary equation of state for the  $\Lambda$  component  $w(z) = w_0 + w_a z/(1+z)$ . In this formula,  $H_0(z)$  can be interpreted as a 'running' current-time Hubble value,

which depends on the redshift of the data used to estimate it. These authors are able to bring the value of  $H_0$  at z=1,100 within  $1\sigma$  of the Planck measurements, hence effectively removing the  $H_0$  tension. However, unlike our approach, where the function F(z) has a well-defined astrophysical interpretation, the use of  $H_0(z)$  and w(z) in Ref. [110] represents ad hoc parametrizations, with their underlying nature remaining unknown. Additionally, the  $H_0(z)$  in Ref. [110] is likely of a cosmic origin, whereas the equation of state w(z) of the  $\Lambda$  component is of a field theoretical origin.

In closing of this section, our study offers a potential resolution to the  $H_0$  tension. Furthermore, it suggests that this tension has an astronomical origin, arising from the growth in the local scale of gravitationally-bound galaxies over cosmic time.

## XI. DISCUSSIONS AND SUMMARY

This paper was inspired by three separate lines of development:

1. In 2003, Blanchard et al (BDRS) proposed a novel CMB analysis that avoids the  $\Lambda$  component [4]. Based solely on the EdS model (i.e.,  $\Omega_{\Lambda}=0$ ) and adopting a double-power primordial fluctuation spectrum, BDRS achieved an excellent fit to WMAP's CMB power spectrum. Surprisingly, they obtained a new value  $H_0\approx 46$ , representing a 34% reduction compared to the accepted value  $H_0\sim 70$  that relies on the flat  $\Lambda$ CDM model with  $\Omega_{\Lambda}\approx 0.7$ .

As independently reported more recently in [102], there exists a strong degeneracy inherent in the parameter space concerning the CMB data. Drawn from this observation, we can interpret BDRS's findings as indicating that within the flat  $\Lambda$ CDM model, the parameter pairs  $\{\Omega_{\Lambda}=0, H_0\approx 46\}$  and  $\{\Omega_{\Lambda}\approx 0.7, H_0\approx 70\}$  are 'nearly degerenate' insofar as the CMB power spectrum is concerned. With a modest modification to the primordial fluctuation spectrum, the BDRS parameter pair  $\{\Omega_{\Lambda}=0, H_0\approx 46\}$  becomes advantageous over the  $\Lambda$ CDM pair  $\{\Omega_{\Lambda}\approx 0.7, H_0\approx 70\}$ . While the cost of this modification is not prohibitive, as BDRS provided justifications in support of a double-power primordial fluctuation spectrum, the benefit is profound in that the DE hypothesis is rendered unnecessary.

This perspective raises an intriguing possibility that the parameter pairs  $\{\Omega_{\Lambda}=0, H_0\approx 46\}$  and  $\{\Omega_{\Lambda}\approx 0.7, H_0\approx 70\}$  may also be 'nearly degenerate' insofar as the Hubble diagram of SNeIa is concerned. To materialize this possibility, one must first seek an alternative approach to late-time acceleration that does not invoke DE. We should emphasize that such an alternative—if it exists—must not only eliminate the role of  $\Omega_{\Lambda}$  but also reduce the  $H_0$  value from  $\sim 70$  to  $\sim 46$ . This presents a stringent requirement to be met.

- 2. A recent theoretical approach developed by the present author [6] induces a variation in the speed of light c (and a variation in the quantum of action  $\hbar$ ) from a dynamical dilaton  $\chi$ . The derivation applies to a class of scale-invariant actions that allow matter to couple with the dilaton. The dynamics of c (and  $\hbar$ ) stems parsimoniously from the dilaton, rather than as serving as an auxiliary addition to the action. The dependencies are determined to be  $c \propto \chi^{1/2}$  and  $\hbar \propto \chi^{-1/2}$ . It was also found that the timescale  $\tau$  and lengthscale l of a given physical process are related in the an anisotropic fashion,  $\tau \propto l^{3/2}$ . See Section II.
- 3. Existing efforts in the literature to apply variable speed of light (VSL) theories to the Hubble diagram of SNeIa have been impeded by a detrimental oversight. All available VSL analyses to date have relied on the standard Lemaître redshift relation,  $1+z=a^{-1}$ , leading to a flawed consensus that VSL plays no role in late-time acceleration. This error stems from the assumption that c is solely a function of cosmic time t, overlooking the possibility that c can vary across the boundaries of galaxies, where a gravitationally-bound galactic region merges with the expanding intergalactic space surrounding it.

In this paper, we build upon the VSL theory referenced in Point #2, correct the error mentioned in Point #3, and reanalyze the Pantheon Catalog. The effects of VSL modify the Lemaître formula to  $1+z=a^{-3/2}$ , with the 3/2-exponent arising from the anisotropic time scaling referenced earlier,  $\tau \propto l^{3/2}$ . Intuitively, this factor 3/2 influences the evaluation of  $H_0$ , resulting in a reduction from the canonical value of  $H_0 \sim 70$  by a factor of 3/2 to  $H_0 = 47.2$ . The new value is compatible with BDRS's findings for the CMB mentioned in Point #1.

**Our derivation and analysis:** The logical steps of our work are as follows.

(i) Modifying the FLRW metric. The universe is modeled as an EdS spacetime supporting a varying c as (see Eq. (20))

$$\begin{cases} ds^2 &= c^2(a) dt^2 - a^2(t) \left[ dr^2 + r^2 d\Omega^2 \right] \\ c(a) &= c_0 \left( \frac{a}{a_0} \right)^{-1/2} \end{cases}$$

with the expansion obeying the growth law  $a(t) = a_0 (t/t_0)^{2/3}$ , see Eq. (17). Justifications for this model are provided in Section III B.

(ii) Modifying the Lemaître redshift formula. Across the boundaries of galaxies, c also varies, leading to a refraction on the lightwaves. Due to this effect, we find that the classic Lemaître redshift formula  $1 + z = a^{-1}$  is inapplicable for the VSL cosmology, and is replaced by the modified Lemaître redshift formula (see Eq. (35))

$$1 + z = a^{-3/2} F^{3/2}(z)$$

with a new exponent of 3/2 and F(z) measuring the relative change in the local scale of galaxies. See Sections III C, IV and V A.

(iii) Modifying the Hubble law. The 3/2-exponent in the modified Lemaître redshift formula above leads to the modified Hubble law (see Eq. (39))

$$z = \frac{3}{2}H_0 \frac{d}{c_0}$$

This new Hubble law differs from the classic Hubble law by a multiplicative factor of 3/2, resulting in a reduction in the  $H_0$  estimate by a factor of 3/2. See Section V B.

(iv) Modifying the luminosity distance-vs-z formula: This formula is the centerpiece of our study (see Eq. (52))

$$\frac{\hat{d}_L}{\hat{c}_{ob}} = \frac{1+z}{H_0 F(z)} \ln \frac{(1+z)^{2/3}}{F(z)}$$

See Sections VC and VD for derivation.

- (v) A re-analysis of the Pantheon data based on VSL: In Section VI, we apply the Formulae above to the Combined Pantheon Sample of SNeIa. We produce an excellent fit without invoking the  $\Lambda$  component; the fit is as robust as that obtained from the  $\Lambda CDM$  model. The optimal values for the parameters are:
  - The Hubble constant  $H_0 = 47.22 \pm 0.4$  (95% CL). This value of consistent with the 3/2 reduction referenced in Point (iii) above.
  - The local scale of galaxies decreases with respect to redshift as  $F(z)=1-(1-F_{\infty}).\left(1-(1+z)^{-2}\right)^2$ , with  $F_{\infty}=0.931\pm0.11$  (95% CL).

Our modified Lemaître redshift formula, Eq. (35), can also effectively viewed as a form of "redshift remapping", a technique advocated in Refs. [111–113]. Interestingly, our value of  $H_0 = 47.2 \pm 0.4$  aligns with the result  $H_0 = 48 \pm 2$  reported in [113].

**Implications:** Four important findings emerge from our analysis.

I) Declining speed of light as an alternative interpretation of the Hubble diagram of SNeIa. At high redshift, the luminosity distance in an EdS universe behaves as  $d_L \propto z$ , whereas in our VSL cosmology, it behaves as  $d_L \propto z \ln z$ . Due to VSL, high-redshift SNeIa thus benefit from the additional  $\ln z$  term, making them appear dimmer than predicted by the EdS model. Another intuitive way to understand this behavior is to note that since  $c \propto a^{-1/2}$ , light traveled faster in the past than in later epochs. As a result, lightwaves from distant SNeIa require less time to traverse the earlier sections of their trajectories, hence experiencing less cosmic expansion (and redshift) than the EdS model predicts. Hence,

the high-z section of the Hubble diagram of SNeIa can be explained—qualitatively and quantitatively—by a declining speed of light rather than a recent cosmic acceleration. A detailed exposition is given in Section VII.

- II) Reviving BDRS's work on the CMB, avoiding dark energy. Despite the very different natures of the data involved, our VSL-based analysis of SNeIa and BDRS's work on the CMB fully agree on two aspects: (i) the universe obeys the EdS model (i.e.  $\Omega_{\Lambda}=0$ ), and (ii)  $H_0$  is reduced to 46–47. The BDRS parameter pair  $\{\Omega_{\Lambda}=0,H_0\approx 46\}$  is advantageous over the  $\Lambda$ CDM pair  $\{\Omega_{\Lambda}\approx 0.7,H_0\approx 70\}$  regarding both the CMB and SNeIa, which are 'orthogonal' datasets. Detailed discussions are presented in Section VIII. Together, our current work and BDRS's 2003 analysis challenge the existence of dark energy—one of the foundational assumptions of the cosmological concordance model.
- III) Resolving the age problem. The age of an EdS universe is given by:  $t_0 = 2/(3H_0)$ . Using the reduced value of  $H_0 = 47.22 \pm 0.4$  km/s/Mpc, one obtains  $t_0 = 13.82 \pm 0.11$  billion years. The age problem is thus resolved through the reduction in  $H_0$ , without requiring a recent acceleration phase induced by dark energy. See Section IX.
- **IV)** Addressing the  $H_0$  tension. Utilizing the function F(z), we recast the current-time Hubble constant as a function  $H_0(z)$  of redshift. Between z=0 and  $z\to\infty$ , the 'running'  $H_0(z)$  exhibits a 7% decrease, a reduction in similar magnitude with the ongoing  $H_0$  tension between the CMB and SNeIa. See Section X.

## On the cosmological time dilation extracted from the Dark Energy Survey (DES)

A recent paper [114] using DES supernova light curves showed no deviation from the relation  $\Delta t_{obs} = \Delta t_{em}(1+z)$ . However, this finding does not contradict our modified Lemaitre redshift formula,  $1+z=a^{-3/2}F(z)$ . This is because the result in Ref. [114] only verifies that the speed of light *inside* the galaxies hosting the supernovae and that *inside* the Milky Way are approximately the same. Galaxies are gravitationally bound and thus not subject to cosmic expansion. Reference [114] does not deal with the speed of light in the intergalactic space, the expansion of which causes c to decline over time. We clarified this distinction in Section IV.

#### XII. CONCLUSION

The nearly identical agreement of the CMB and SNeIa regarding the reduced value of  $H_0 \sim 46$ –47 is highly encouraging. This alignment points toward a consistent cosmological framework based on the Einstein–de Sitter model with a variable speed of light, thus eliminating the

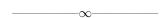
need for dark energy and dissolving its fine-tuning and coincidence problems.

Importantly, we have built a case for an alternative perspective: rather than supporting a  $\Lambda$ CDM universe undergoing late-time acceleration, the Hubble diagram of SNeIa can be reinterpreted as evidence for a declining speed of light in an expanding Einstein-de Sitter universe.

Finally, we note that the observational bounds established in the literature in support of a constant speed of light have predominantly relied on standard cosmology [34–38, 42–46, 62, 63, 67, 69, 70, 73, 84]. However, our new Lemaître redshift formula represents a critical departure from this conventional framework. Therefore, the consensus regarding the absence of variation in c in observational cosmology must be reconsidered in light of our findings, prompting a comprehensive reanalysis of these constraints.

#### ACKNOWLEDGMENTS

I thank Clifford Burgess, Tiberiu Harko, Robert Mann, Anne-Christine Davis, Eoin Ó Colgáin, Demosthenes Kazanas, Leandros Perivolaropoulos, Alberto Salvio, Ilya L. Shapiro, John Moffat, Gregory Volovik and Bruce Bassett for their constructive and insightful feedback.



## Appendix A: Refraction effect

Let us start with a well-understood phenomenon: the behavior of a wavetrain in a medium with varying speed of wave. It is well established that the wavelength of the wavetrain at a given location is proportional to the speed of wave at that location:

$$\lambda \propto v$$
 (A1)

Figure 10 illustrates the change in wavelength as a wave travels at varying speed. In the upper panel, as the speed increases, the front end of the wavecrest will rush forward leaving its back end behind thus stretching out the wavecrest. In the lower panel, the reverse situation occurs: as the speed decreases, the front end of the wavecrest will slow down while its back end continues its course thus compressing the wavecrest. In either situation, the wavelength and the speed of wave are directly proportional:

$$\frac{\lambda_2}{\lambda_1} = \frac{v_2}{v_1} \tag{A2}$$

Note that the details of how the variation of v does not participate in formula above.

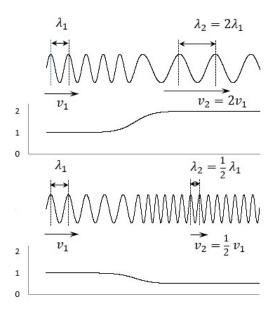


Figure 10. Change in wavelength as a wavetrain travels in a medium with varying speed of wave. Upper panel: wavelength doubles as its speed doubles. Lower panel: wavelength halves as its speed halves. In either case, wavelength and speed are proportional:  $\lambda_2/v_2 = \lambda_1/v_1$ .

# Appendix B: An equivalent derivation of the modified Lemaître redshift formula

We produce an alternative route by way of frequency transformation to modifying Lemaître's redshift formula (35). We have derived in Eq. (25) that

$$\frac{\nu_{ob}}{\nu_{em}} = \frac{a_{em}^{3/2}}{a_{ob}^{3/2}} \tag{B1}$$

For transits between local regions to global regions (i.e., Transit #1 and Transit #3 in Fig. 1 in Page 6), since  $\lambda \propto c$ , the frequency is:

$$\nu = \frac{c}{\lambda} = \text{const} \tag{B2}$$

This means that the frequency of the lightwave does not change during Transit #1 and Transit #3, viz.

$$\hat{\nu}_{em} = \nu_{em}; \quad \hat{\nu}_{ob} = \nu_{ob} \tag{B3}$$

Given that

$$\hat{\lambda}_{ob} = \frac{\hat{c}_{ob}}{\hat{\nu}_{ob}}; \quad \hat{\lambda}_{em} = \frac{\hat{c}_{em}}{\hat{\nu}_{em}}; \quad \frac{\lambda^*}{\hat{\lambda}_{em}} = \frac{\hat{a}_{ob}}{\hat{a}_{em}}$$
(B4)

and

$$\frac{\hat{c}_{ob}}{\hat{c}_{em}} = \frac{\hat{a}_{ob}^{-1/2}}{\hat{a}_{em}^{-1/2}} \tag{B5}$$

it is straightforward to verify that

$$1 + z = \frac{\hat{\lambda}_{ob}}{\lambda^*} = \frac{a_{ob}^{3/2}}{a_{em}^{3/2}} \frac{\hat{a}_{em}^{3/2}}{\hat{a}_{ob}^{3/2}}$$
(B6)

a relation that is in perfect agreement with Eq. (35).

- [1] L. Perivolaropoulos and F. Skara, Challenges for ACDM: An update, New Astron. Rev. 95, 101659 (2022), arXiv:2105.05208 [astro-ph.CO]
- [2] E. Di Valentino, O. Mena, S. Pan, L. Visinelli, W. Yang, A. Melchiorri, D. F. Mota, A. G. Riess and J. Silk, In the realm of the Hubble tension—a review of solutions, Class. Quant. Grav. 38 (2021) no.15, 153001, arXiv:2103.01183 [astro-ph.CO]
- [3] P. Bull, Y. Arkrami, et al, Beyond ACDM: Problems, solutions, and the road ahead, Physics of the Dark Universe 12 (2016) 56, arXiv:1512.05356
- [4] A. Blanchard, M. Douspis, M. Rowan-Robinson and S. Sarkar, An alternative to the cosmological "concordance model", Astron. Astrophys. 412, 35-44 (2003), arXiv:astro-ph/0304237
- [5] P. Hunt and S. Sarkar, Multiple inflation and the WMAP "glitches". II. Data analysis and cosmological parameter extraction, Phys. Rev. D 76, 123504 (2007), arXiv:0706.2443 [astro-ph]
- [6] H. K. Nguyen, Dilaton-induced variations in Planck constant and speed of light: An alternative to Dark Energy, Phys. Lett. B 862 (2025) 139357, arXiv:2412.04257 [gr-qc]
- [7] H. K. Nguyen, A mechanism to generate varying speed of light via Higgs-dilaton coupling: Theory and cosmological applications, to appear in Eur. Phys. J. C, arXiv:2408.02583 [gr-qc]
- [8] A. Einstein, On the influence of gravitation on the propagation of light, Annalen der Physik 35, 898-908 (1911),
   Link to English translation
- [9] A. Einstein, The speed of light and the statics of the gravitational field, Annalen der Physik 38, 355-369 (1912), Link to English translation
- [10] A. Einstein, Relativity and gravitation: Reply to a comment by M. Abraham, Annalen der Physik 38, 1059-1064 (1912), Link to English translation
- [11] R. H. Dicke, Gravitation without a Principle of Equivalence, Rev. Mod. Phys. 29, 363 (1957)
- [12] C. H. Brans and R. Dicke, Mach's Principle and a relativistic theory of gravitation, Phys. Rev. 124, 925 (1961)
- [13] J. W. Moffat, Superluminary universe: A possible solution to the initial value problem in cosmology, Int. J. Mod. Phys. D 2, 351 (1993), arXiv:gr-qc/9211020
- [14] A. Albrecht and J. Magueijo, Time varying speed of light as a solution to cosmological puzzles, Phys. Rev. D 59, 043516 (1999), arXiv:astro-ph/9811018
- [15] J. D. Barrow, Cosmologies with varying light speed, Phys. Rev. D 59, 043515 (1999), arXiv:astroph/9811022
- [16] J. D. Barrow and J. Magueijo, Varying-α theories and solutions to the cosmological problems, Phys. Lett. B 443, 104 (1998), arXiv:astro-ph/9811072
- [17] J. D. Barrow and J. Magueijo, Can a changing a explain

- the Supernovae results?, Astrophys. J. **532**, L87–L90 (2000), arXiv:astro-ph/9907354
- [18] J. Magueijo and L. Smolin, Lorentz invariance with an invariant energy scale, Phys. Rev. Lett. 88, 190403 (2002), arXiv:hep-th/0112090
- [19] J. Magueijo, New varying speed of light theories, Rept. Prog. Phys. 66, 2025 (2003), arxiv:astro-ph/0305457
- [20] J. D. Barrow and J. Magueijo, Solutions to the Quasiflatness and Quasi-lambda Problems, Phys. Lett. B 447, 246 (1999), arXiv:astro-ph/9811073
- [21] J. D. Barrow and J. Magueijo, Solving the Flatness and Quasi-flatness Problems in Brans-Dicke Cosmologies with a Varying Light Speed, Class. Quant. Grav. 16, 1435 (1999), arXiv:astro-ph/9901049
- [22] M. A. Clayton and J. W. Moffat, Dynamical mechanism for varying light velocity as a solution to cosmological problems, Phys. Lett. B 460, 263 (1999), arXiv:astroph/9812481 [astro-ph]
- [23] P. P. Avelino and C. J. A. P. Martins, Does a varying speed of light solve the cosmological problems?, Phys. Lett. B 459 (1999), 468-472, arXiv:astro-ph/9906117 [astro-ph]
- [24] P. P. Avelino, C. J. A. P. Martins and G. Rocha, VSL theories and the Doppler peak, Phys. Lett. B 483 (2000) 210, arXiv:astro-ph/0001292
- [25] M. A. Clayton and J. W. Moffat, Scalar tensor gravity theory for dynamical light velocity, Phys. Lett. B 477 (2000), 269-275, arXiv:gr-qc/9910112 [gr-qc]
- [26] J. Magueijo, Covariant and locally Lorentz invariant varying speed of light theories, Phys. Rev. D 62 (2000), 103521, arXiv:gr-qc/0007036
- [27] M. A. Clayton and J. W. Moffat, Vector field mediated models of dynamical light velocity, Int. J. Mod. Phys. D 11 (2002), 187-206, arXiv:gr-qc/0003070 [gr-qc]
- [28] B. A. Bassett, S. Liberati, C. Molina-Paris and M. Visser, Geometrodynamics of Variable-Speed-of-Light Cosmologies, Phys. Rev. D 62, 103518 (2000), arXiv:astro-ph/0001441
- [29] S. Liberati, B. A. Bassett, C. Molina-Paris and M. Visser, Chi-Variable-Speed-of-Light Cosmologies, Nucl. Phys. Proc. Suppl. 88, 259 (2000), arXiv:astro-ph/0001481
- [30] I. T. Drummond, Variable Light-Cone Theory of Gravity, arXiv:gr-qc/9908058
- [31] I. T. Drummond and S. J. Hathrell, QED vacuum polarization in a background gravitational field and its effect on the velocity of photons, Phys. Rev. D 22, 343 (1980)
- [32] M. Novello and S. D. Jorda, Does there exist a cosmological horizon problem?, Mod. Phys. Lett. A 4, 1809 (1989)
- [33] G. E. Volovik, Planck constants in the symmetry breaking quantum gravity, Symmetry 15, 991 (2023), arXiv:2304.04235 [cond-mat.other]

- [34] P. Zhang and X. Meng, SNe data analysis in variable speed of light cosmologies without cosmological constant, Mod. Phys. Lett. A Vol. 29, No. 24, 1450103 (2014), arXiv:1404.7693 [astro-ph.CO]
- [35] J-Z. Qi, M-J. Zhang and W-B. Liu, Observational constraint on the varying speed of light theory, Phys. Rev. D 90, 063526 (2014), arXiv:1407.1265 [gr-qc]
- [36] A. Ravanpak, H. Farajollahi and G.F. Fadakar, Normal DGP in varying speed of light cosmology, Res. Astron. Astrophys. 17, 26 (2017), arXiv:1703.09811
- [37] V. Salzano and M. P. Dabrowski, Statistical hierarchy of varying speed of light cosmologies, Astrophys. J. 851, 97 (2017), arXiv:1612.06367
- [38] A. Balcerzak, M. P. Dabrowski and V. Salzano, Modelling spatial variations of the speed of light, Annalen der Physik 29, 1600409 (2017), arXiv:1604.07655 [astroph.CO]
- [39] R. P. Gupta, Cosmology with relativistically varying physical constants, Mon. Not. Roy. Astron. Soc. 498 (2020) 3, 4481-4491, arXiv:2009.08878 [astro-ph.CO]
- [40] R. P. Gupta, Varying physical constants and the lithium problem, Astroparticle Physics 129, 102578 (2021), arXiv:2010.13628 [gr-qc]
- [41] R. R. Cuzinatto, R. P. Gupta, R. F. L. Holanda, J. F. Jesus and S. H. Pereira, Testing a varying-A model for dark energy within Co-varying Physical Couplings framework, Mon. Not. Roy. Astron. Soc. 515, 5981-5992 (2022), arXiv:2204.10764 [gr-qc]
- [42] A. A. Abdo et al, A limit on the variation of the speed of light arising from quantum gravity effects, Nature 462, 331-334 (2009)
- [43] R. Agrawal, H. Singirikonda and S. Desai, Search for Lorentz Invariance Violation from stacked Gamma-Ray Burst spectral lag data, JCAP 05 (2021) 029, arXiv:2102.11248 [astro-ph.HE]
- [44] J. Santos, C. Bengaly, B. J. Morais and R. S. Goncalves, Measuring the speed of light with cosmological observations: current constraints and forecasts, JCAP 11 (2024) 062, arXiv:2409.05838 [astro-ph.CO]
- [45] J. P. Uzan, The Fundamental Constants and Their Variation: Observational Status and Theoretical Motivations, Rev. Mod. Phys. 75 (2003), 403, arXiv:hepph/0205340 [hep-ph]
- [46] J. P. Uzan, Varying Constants, Gravitation and Cosmology, Living Rev. Rel. 14 (2011), 2, arXiv:1009.5514 [astro-ph.CO]
- [47] C. J. A. P. Martins, The status of varying constants: a review of the physics, searches and implications, Rep. Prog. Phys. 80, 126902 (2017), arXiv:1709.02923 [astro-ph.CO]
- [48] G. F. R. Ellis and J. P. Uzan, 'c' is the speed of light, isn't it?, Am. J. Phys. 73 (2005), 240-247, arXiv:gr-qc/0305099 [gr-qc]
- [49] G. F. R. Ellis, Note on Varying Speed of Light Cosmologies, Gen. Rel. Grav. 39 (2007), 511-520, arXiv:astro-ph/0703751 [astro-ph] https://arxiv.org/abs/astro-ph/0703751
- [50] J. Magueijo and J. W. Moffat, Comments on "Note on varying speed of light theories", Gen. Rel. Grav. 40, 1797-1806 (2008), arXiv:0705.4507
- [51] A. Buchalter, On the time variation of c, G, and h and the dynamics of the cosmic expansion, arXiv:astroph/0403202
- [52] C. N. Cruz and A. C. A. de Faria Jr., Variation of the

- speed of light with temperature of the expanding universe, Phys. Rev. D **86** (2012), 027703, arXiv:1205.2298 [gr-qc]
- [53] J. W. Moffat, Variable Speed of Light Cosmology, Primordial Fluctuations and Gravitational Waves, Eur. Phys. J. C 76, 130 (2016), arXiv:1404.5567 [astroph.CO]
- [54] G. Franzmann, Varying fundamental constants: a full covariant approach and cosmological applications, arXiv:1704.07368 [gr-qc]
- [55] C. N. Cruz and F. A. da Silva, Variation of the speed of light and a minimum speed in the scenario of an inflationary universe with accelerated expansion, Phys. Dark Univ. 22 (2018), 127-136, arXiv:2009.05397 [physics.gen-ph]
- [56] R. Costa, R. R. Cuzinatto, E. M. G. Ferreira and G. Franzmann, Covariant c-flation: a variational approach, Int. J. Mod. Phys. D 28, 1950119 (2019), arXiv:1705.03461 [gr-qc]
- [57] S. Lee, The minimally extended Varying Speed of Light (meVSL), JCAP 08 (2021), 054, arXiv:2011.09274 [astro-ph.CO]
- [58] A. Balcerzak and M. P. Dabrowski, Redshift drift in varying speed of light cosmology, Phys. Lett. B 728 (2014), 15, arXiv:1310.7231 [astro-ph.CO]
- [59] A. Balcerzak and M. P. Dabrowski, A statefinder luminosity distance formula in varying speed of light cosmology, JCAP 06 (2014), 035, arXiv:1406.0150 [astroph.CO]
- [60] V. Salzano, M. P. Dabrowski and R. Lazkoz, Measuring the speed of light with Baryon Acoustic Oscillations, Phys. Rev. Lett. 114, 101304 (2015), arXiv:1412.5653 [astro-ph.CO]
- [61] V. Salzano, M. P. Dabrowski and R. Lazkoz, Probing the constancy of the speed of light with future galaxy survey: The case of SKA and Euclid, Phys. Rev. D 93, 063521 (2016), arXiv:1511.04732 [astro-ph.CO]
- [62] R. G. Cai, Z. K. Guo and T. Yang, Dodging the cosmic curvature to probe the constancy of the speed of light, JCAP 08 (2016), 016, arXiv:1601.05497 [astro-ph.CO]
- [63] S. Cao, M. Biesiada, J. Jackson, X. Zheng, Y. Zhao and Z. H. Zhu, Measuring the speed of light with ultra-compact radio quasars, JCAP 02 (2017), 012, arXiv:1609.08748 [astro-ph.CO]
- [64] V. Salzano, How to Reconstruct a Varying Speed of Light Signal from Baryon Acoustic Oscillations Surveys, Universe 3 (2017) no.2, 35
- [65] V. Salzano, Recovering a redshift-extended VSL signal from galaxy surveys, Phys. Rev. D 95, 084035 (2017), arXiv:1604.03398 [astro-ph.CO]
- [66] R. G. Lang, H. Martinez-Huerta and V. de Souza, Limits on the Lorentz Invariance Violation from UHECR astrophysics, Astrophys. J. 853 (2018) no.1, 23, arXiv:1701.04865 [astro-ph.HE]
- [67] X. B. Zou, H. K. Deng, Z. Y. Yin and H. Wei, Model-Independent Constraints on Lorentz Invariance Violation via the Cosmographic Approach, Phys. Lett. B 776 (2018), 284-294, arXiv:1707.06367 [gr-qc]
- [68] H. Martinez-Huerta [HAWC], Potential constrains on Lorentz invariance violation from the HAWC TeV gamma-rays, PoS ICRC2017 (2018), 868, arXiv:1708.03384 [astro-ph.HE]
- [69] S. Cao, J. Qi, M. Biesiada, X. Zheng, T. Xu and Z. H. Zhu, Testing the Speed of Light over Cosmological Dis-

- tances: The Combination of Strongly Lensed and Unlensed Type Ia Supernovae, Astrophys. J. **867** (2018) no.1, 50, arXiv:1810.01287 [astro-ph.CO]
- [70] D. Wang, H. Zhang, J. Zheng, Y. Wang and G. B. Zhao, Reconstructing the temporal evolution of the speed of light in a flat FRW Universe, Res. Astron. Astrophys. 19 (2019) 10, 152, arXiv:1904.04041 [astro-ph.CO]
- [71] A. Albert et al. [HAWC], Constraints on Lorentz Invariance Violation from HAWC Observations of Gamma Rays above 100 TeV, Phys. Rev. Lett. 124 (2020) no.13, 131101, arXiv:1911.08070 [astroph.HE]
- [72] Y. Pan, J. Qi, S. Cao, T. Liu, Y. Liu, S. Geng, Y. Lian and Z. H. Zhu, Model-independent constraints on Lorentz invariance violation: implication from updated Gamma-ray burst observations, Astrophys. J. 890 (2020), 169, arXiv:2001.08451 [astro-ph.CO]
- [73] I. E. C. R. Mendonca, K. Bora, R. F. L. Holanda, S. Desai and S. H. Pereira, A search for the variation of speed of light using galaxy cluster gas mass fraction measurements, JCAP 11 (2021), 034, arXiv:2109.14512 [astroph.CO]
- [74] G. Rodrigues and C. Bengaly, A model-independent test of speed of light variability with cosmological observations, JCAP 07 (2022) no.07, 029, arXiv:2112.01963 [astro-ph.CO]
- [75] S. Lee, Constraining minimally extended varying speed of light by cosmological chronometers, Mon. Not. Roy. Astron. Soc. 522 (2023) no.3, 3248-3255, arXiv:2301.06947 [astro-ph.CO]
- [76] R. E. Eaves, Redshift in varying speed of light cosmology, Mon. Not. Roy. Astron. Soc. 516, 4136–4145 (2022)
- [77] P. Mukherjee, G. Rodrigues and C. Bengaly, Examining the validity of the minimal varying speed of light model through cosmological observations: Relaxing the null curvature constraint, Phys. Dark Univ. 43 (2024), 101380, arXiv:2302.00867 [astro-ph.CO]
- [78] Y. Liu, S. Cao, M. Biesiada, Y. Lian, X. Liu and Y. Zhang, Measuring the Speed of Light with Updated Hubble Diagram of High-redshift Standard Candles, Astrophys. J. 949 (2023) no.2, 57, arXiv:2303.14674 [astroph.CO]
- [79] S. Lee, Constraint on the minimally extended varying speed of light using time dilations in Type Ia supernovae, Mon. Not. Roy. Astron. Soc. 524 (2023) no.3, 4019-4023, arXiv:2302.09735 [astro-ph.CO]
- [80] S. Lee, Constraints on the time variation of the speed of light using Strong lensing, arXiv:2104.09690 [astroph.CO]
- [81] R. R. Cuzinatto, C. A. M. de Melo and J. C. S. Neves, Shadows of black holes at cosmological distances in the co-varying physical couplings framework, Mon. Not. Roy. Astron. Soc. 526 (2023) no.3, 3987-3993, arXiv:2305.11118 [gr-qc]
- [82] C. Y. Zhang, W. Hong, Y. C. Wang and T. J. Zhang, A Stochastic Approach to Reconstructing the Speed of Light in Cosmology, Mon. Not. Roy. Astron. Soc. 534 (2024), 56-69, arXiv:2409.03248 [astro-ph.CO]
- [83] T. Liu, S. Cao, M. Biesiada, Y. Liu, Y. Lian and Y. Zhang, Consistency testing for invariance of the speed of light at different redshifts: the newest results from strong lensing and Type Ia supernovae observations, Mon. Not. Roy. Astron. Soc. 506 (2021) 2, 2181-2188, arXiv:2106.15145 [astro-ph.CO]
- [84] L. R. Colaco, S. J. Landau, J. E. Gonzalez, J. Spinelly

- and G. L. F. Santos, Constraining a possible timevariation of the speed of light along with the finestructure constant using strong gravitational lensing and Type Ia supernovae observations, JCAP **08** (2022) 062, arXiv:2204.06459 [astro-ph.CO]
- [85] Y. Liu and B-Q. Ma, Light speed variation from gamma ray bursts: criteria for low energy photons, Eur. Phys. J. C 78 (2018) 825, arXiv:1810.00636 [astro-ph.HE]
- [86] H. Xu and B-Q. Ma, Light speed variation from gamma-ray bursts, Astropart. Phys. 82, 72 (2016), arXiv:1607.03203 [hep-ph]
- [87] H. Xu and B-Q. Ma, Light speed variation from gamma ray burst GRB 160509A, Phys. Lett. B 760 (2016) 602-604, arXiv:1607.08043 [hep-ph]
- [88] J. Zhu and B-Q. Ma, Pre-burst events of gamma-ray bursts with light speed variation, Phys. Lett. B 820 (2021) 136518, arXiv:2108.05804 [astro-ph.HE]
- [89] D. Blas, M. Shaposhnikov and D. Zenhausern, Scale-invariant alternatives to general relativity, Phys. Rev. D 84, 044001 (2011), arXiv:1104.1392 [hep-th]
- [90] P. G. Ferreira, C. T. Hill and G. G. Ross, No fifth force in a scale invariant universe, Phys. Rev. D 95, 064038 (2017), arXiv:1612.03157 [gr-qc]
- [91] Y. Fujii, Origin of the gravitational constant and particle masses in scale invariant scalar-tensor theory, Phys. Rev. D 26, 2580 (1982)
- [92] C. Wetterich, Cosmologies with variable Newton's 'constant', Nucl. Phys. B 302, 645 (1988)
- [93] C. Wetterich, Cosmology and the fate of dilatation symmetry, Nucl. Phys. B 302, 668 (1988), arXiv:1711.03844 [hep-th]
- [94] C. Wetterich, Variable gravity Universe, Phys. Rev. D 89, 024005 (2014), arXiv:1308.1019 [astro-ph.CO]
- [95] D. M. Scolnic et al, The complete light-curve sample of spectroscopically confirmed Type Ia supernovae from Pan-STARRS1 and cosmological constraints from the Combined Pantheon Sample, Astrophys. J. 859 (2018) 2, 101, arXiv:1710.00845 [astro-ph.CO]
- [96] We used the following data file: archive.stsci.edu/hlsps /ps1cosmo/scolnic/data\_fitres/hlsp\_ps1cosmo\_panstarrs\_ gpc1\_all\_model\_v1\_ancillary-g10.fitres
- [97] A. Riess et al, Observational evidence from supernovae for an accelerating universe and a cosmological constant, Astron. J. 116, 1009 (1998), arXiv:astro-ph/9805201
- [98] S. Perlmutter et al, Measurements of  $\Omega$  and  $\Lambda$  from 42 high-redshift supernovae, Astron. J. **517**, 565 (1999), arXiv:astro-ph/9812133
- [99] P. A. R. Ade et al. [Planck], Planck 2015 results. XIII. Cosmological parameters, Astron. Astrophys. 594 (2016) A13, arXiv:1502.01589 [astro-ph.CO]
- [100] P. A. R. Ade et al. [Planck], Planck 2015 results. XX. Constraints on inflation, Astron. Astrophys. 594 (2016) A20, arXiv:1502.02114 [astro-ph.CO]
- [101] T. Shanks, Problems with the Current Cosmological Paradigm, IAU Symp. 216, 398 (2005), arXiv:astroph/0401409
- [102] G. Alestas, L. Kazantzidis and L. Perivolaropoulos, H<sub>0</sub> Tension, Phantom Dark Energy and Cosmological Parameter Degeneracies, Phys. Rev. D 101, 123516 (2020), arXiv:2004.08363 [astro-ph.CO]
- [103] D. J. Eisenstein et al, Detection of the Baryon Acoustic Peak in the Large-Scale Correlation Function of SDSS Luminous Red Galaxies, Astrophys. J. 633, 560 (2005), arXiv:astro-ph/0501171

- [104] A. Blanchard, M. Douspis, M. Rowan-Robinson and S. Sarkar, Large-scale galaxy correlations as a test for dark energy, Astron. Astrophys. 449, 925 (2006), arXiv:astro-ph/0512085
- [105] E.g., see D. S. Gorbunov and V. A. Rubakov, Introduction to the Theory of the Early Universe: Hot big bang theory, Word Scientific (2011), page 68
- [106] K. Ormerod, C. J. Conselice, N. J. Adams, T. Harvey, D. Austin, J. Trussler, L. Ferreira, J. Caruana, G. Lucatelli, Q. Li and W. J. Roper, EPOCHS VI: the size and shape evolution of galaxies since z ~ 8 with JWST Observations, Mon. Not. Roy. Astron. Soc. 527, 6110– 6125 (2024), arXiv:2309.04377 [astro-ph.GA]
- [107] F. Buitrago and I. Trujillo, Strong size evolution of disc galaxies since z = 1: Readdressing galaxy growth using a physically motivated size indicator, Astron. Astrophys. 682, A110 (2024), arXiv:2311.07656 [astro-ph.GA]
- [108] C. Krishnan, E. Ó Colgáin, Ruchika, A. A. Sen, M. M. Sheikh-Jabbari and T. Yang, Is there an early Universe solution to Hubble tension?, Phys. Rev. D 102, 103525 (2020), arXiv:2002.06044 [astro-ph.CO]
- [109] C. Krishnan, E. Ó Colgáin, M. M. Sheikh-Jabbari and

- T. Yang, Running Hubble Tension and a  $H_0$  Diagnostic, Phys. Rev. D **103**, 103509 (2021), arXiv:2011.02858 [astro-ph.CO]
- [110] M. G. Dainotti, B. De Simone, T. Schiavone, G. Montani, E. Rinaldi and G. Lambiase, On the Hubble constant tension in the SNe Ia Pantheon sample, Astrophys. J. 912 (2021) 2, 150, arXiv:2103.02117 [astroph.CO]
- [111] B. A. Bassett, Y. Fantaye, R. Hložek, C. Sabiu and M. Smith, Observational Constraints on Redshift Remapping, arXiv:1312.2593 [astro-ph.CO]
- [112] R. Wojtak and F. Prada, Testing the mapping between redshift and cosmic scale factor, Mon. Not. Roy. Astron. Soc. 458, 3331 (2016), arXiv:1602.02231 [astro-ph.CO]
- [113] R. Wojtak and F. Prada, Redshift remapping and cosmic acceleration in dark-matter-dominated cosmological models, Mon. Not. Roy. Astron. Soc. 470, 4493 (2017), arXiv:1610.03599 [astro-ph.CO]
- [114] R. M. T. White et al [DES Collaboration], The Dark Energy Survey Supernova Program: slow supernovae show cosmological time dilation out to  $z\sim 1$ , Mon. Not. Roy. Astron. Soc. **533** (2024) 3, 3365-3378, arXiv:2406.05050 [astro-ph.CO]